Decoding pain from brain activity

Running title: Decoding pain from brain activity

Figures and Tables: 5 and 4

Abstract

Pain is a dynamic, complex and multidimensional experience. The identification of pain from brain activity as neural readout may effectively provide a neural code for pain, and further provide useful information for pain diagnosis and treatment. Advances in neuroimaging and large-scale electrophysiology have enabled us to examine neural activity with improved spatial and temporal resolution, providing opportunities to decode pain in humans and freely behaving animals. This topical review provides a systematical overview of state-of-the-art methods for decoding pain from brain signals, with special emphasis on electrophysiological and neuroimaging modalities. We will discuss the applications and challenges in the research field, and point to a few future research directions.

Keywords: chronic pain; machine learning; state-space model; unsupervised learning; functional connectivity; brain machine interface; biomarker

1 Introduction

Pain is an unpleasant sensory and emotional experience that signals threat and promotes behavior to protect individuals. Pain perception is heavily influenced by prior experience and expectations of pain (Sawamoto et al., 2000; Koyama et al., 2005), and is dependent on the context (Leknes et al., 2000) and other sensory inputs (Senkowski et al., 2014), as well as multiple contextual, psychological, social, and cultural factors (Leknes et al., 2000). Research during the last 50 years has resulted in a growing understanding of spinal, peripheral and cortical mechanisms for pain (Besson, 1999; Apkarian et al., 2005; Iannetti and Mouraux, 2010; Rosa and Seymour, 2014). Specifically, central neocortical and subcortical neural circuits that regulate pain, especially in the emotional and motivational components of pain, remain incompletely understood. Such understanding, however, is vital to the knowledge of how the brain processes sensory and affective information, and it could lead to novel therapeutic strategies.

Because of the lack of a pain cortex, functional connectivity (FC) of a large brain network or specific cortical-subcortical pain pathways have been investigated in pain studies (Baliki et al., 2012; Necka et al., 2019; Nickel et al., 2020; Barroso et al., 2021). However, most studies are correlational. To fully understand pain, systems-level circuit dissection is required to uncover the causal role of relationship between pain circuits and behavior. In order to find effective pain treatment, neuroscientists and physicians need to first understand the neurobiology of pain, identify the neural correlates of pain, and further establish the causal link between pain behavior and brain signals (Kucyi and Davis, 2017). From a computational perspective, a fundamental question arises: can we reliably decode pain from brain activity? To date, studies have attempted to combine brain imaging, neural signal processing and machine learning (ML) to identify circuit changes that can function as a putative neural code for pain (Brodersen et al., 2012; Wagner et al., 2013; Rosa and Seymour, 2014). This goal is feasible because first, recent advances in neural recording and imaging technologies have provided opportunities for unraveling new research questions and developing new methods. However, as we discuss in the paper, many features of brain activity that are associated with pain are not specific to pain.

Consequently, it remains challenging to make inference whether an animal or individual experience pain without a controlled experimental setup (Davis et al., 2017). Second, from a methodological perspective, ML techniques provide powerful tools for pain research by examining dynamic spatiotemporal patterns of the brain activity (Rosa and Seymour, 2014; Lotsch and Ultsch, 2018).

This paper is aimed to provide a comprehensive review of signal processing and ML methods for detecting pain from brain signals. We will focus on the decoding effort based on dynamic brain activity, while other decoding efforts based on brain structural data (such as grey matter volume and white matter connectivity) are referred to elsewhere (Bagarinao et al., 2014; Ung et al., 2014; Labus et al., 2015; Kuner and Flor, 2016). The remaining paper is organized as follows. In Section 2, we present a brief background on acute and chronic pain. Section 3 discusses the behavioral and neural measurements of pain. Section 4 reviews the supervised and unsupervised methods for pain decoding. Finally, Section 5 concludes the paper with discussion and future research directions.

2 Background of Acute and Chronic Pain

Pain processing typically involves transmission and modulation of nociceptive signals along a pathway (Willis and Westlund, 1997). In the ascending pathway, the nociception originates in the peripheral system, and then passes the signals to the dorsal horn of the spinal cord, then further to the thalamus, and the cortex. The descending system, involving the midbrain, rostral ventromedial medulla (RVM), periaqueductal gray (PAG) and other areas, can exert both inhibitory and modulatory influence.

Pain is known to have three distinct dimensions: sensory-discriminative, affective-motivational, and cognitive-evaluative dimensions (Melzack and Casey, 1969; Wiech et al., 2008). Pain experiences are primarily sensory driven ("evoked"), whereas some pain experiences are internally driven ("spontaneous" or "tonic"). Depending on the duration of pain experiences, pain can be categorized as either acute or chronic. Acute pain is caused by noxious thermal or mechanical stimulations and goes away when there is no longer an underlying cause for the pain, whereas chronic pain is a condition in which pain progresses

from an acute to chronic state and persists beyond the healing process (e.g., >3 months). Furthermore, chronic pain has three major subcategories: nociceptive, neuropathic, and nociplastic pain (Cohen et al., 2021). Nociceptive pain results from the activation of nociceptors sensitive to noxious stimuli; neuropathic pain is caused by dysfunctional nerves, or by nerve disturbances and damage; nociplastic pain is caused by ongoing inflammation and damage of tissues (Cohen et al., 2021; Fitzcharles et al., 2021). Chronic pain affects patients' quality of life and mental health, but the circuit mechanism and complete understanding of chronic pain remain elusive, creating a barrier for effective therapeutic treatment.

Unlike other sensory perception that is uniquely associated with a specific sensory cortex (e.g., visual cortex, auditory cortex or olfactory cortex), there is no a pain cortex associated with pain perception. Instead, pain is associated with the activation of a distributed network of multiple cortical and subcortical areas (Apkarian et al., 2005; Ploner et al., 2017), including the primary somatosensory cortex (S1), secondary somatosensory cortex (S2), anterior cingulate cortex (ACC), prefrontal cortex (PFC), insular cortex, nucleus accumbens (NAc), amygdala and thalamus (Davis et al., 2017; Mouraux and Iannetti, 2018). See Fig. 1A for a graphical illustration of the key "nodes" of the "pain matrix". Neuroimaging studies have advanced the understanding of brain mechanisms in pain, but these studies are limited to be correlational. A complete dissection of pain circuitry relies on optogenetics and electrophysiology using animal models of pain (Lee et al., 2015; Gu et al., 2015; Zhang et al., 2017; Dale et al., 2018; Meda et al., 2019; Tan et al., 2019; Singh et al., 2020). To date, multiple lines of evidence from human neuroimaging and animal electrophysiology have shown that the ACC is engaged in emotional and affective processing of pain (Kuo and Yen, 2005; Bushnell et al., 2013; Zhang et al., 2017), the S1 and S2 are involved in sensory processing of pain (Kuo and Yen, 2005; Vierck et al., 2013; Xiao et al., 2019b), and the insular plays a key multifaceted role in intensity coding and using cognitive information to modulate connected brain areas involved in processing of sensorydiscriminative, affective, and cognitive-evaluative components of pain (Coghill et al., 1999; Starr et al., 2009; Lu et al., 2009).

3 Measurements of Pain

3.1 Measurements of pain behaviors

Pain behaviors are overt, and can be observed and recorded. However, pain perceptions are also highly subjective, behavioral assessments of pain in animals and humans have been developed and evaluated by researchers. In rodent studies, pain behaviors are often characterized by the reaction time (or paw withdrawal time) to noxious stimulations or other self-protective maneuvers (Cheppudira, 2006; Deuis, 2017). For instance, the conditioned place preference (CPA) or conditioned place aversion (CPA) assay are common behavioral tests to measure the pain-related aversion responses. In human pain studies, quantification of pain behaviors depend on the designed task (e.g., reaction time) and/or pain rating (Fordyce et al., 1984). The self-report measures often include self-report pain intensity were assessed using the visual analogue scale (VAS, range: 0-9) (Boonstra et al., 2008). In clinical setting, pain-related measurements also include reductions in physical activity, increased medication intake, or alterations in facial expressions or body posture. For instance, to assess chronic low back pain, the pain behavior scale (PaBS) is aimed to record the presence and severity of pain behaviors exhibited during the physical performance tests. The assessed pain behaviors may include sighing, breath-holding, grimacing, guarding, rubbing, and antalgic gait (Keefe and Block, 1982).

It is known that individuals may exhibit considerable and unpredictable variability in painful percepts in response to the same nociceptive stimulus, and the self-reported pain intensity often poorly correlates with the stimulus intensity. The sources of such within-subject and between-subject variability remain poorly understood. One of the goals of pain decoding is to identify neural correlates or indicators that explain such perceptual variability of pain (Hu and Iannetti, 2019).

3.2 Measurements of brain activity

Advances in neurotechnology has enabled us to record brain signals at both microscopic and macroscopic levels, ranging from neuronal spiking activity to the proxy of brain activity, depending on the trade-off of spatial and temporal resolution (Fig. 1B). Measurements of

neural signals can be either invasive or non-invasive, or something in between ("minimally invasive"). Different sources of electrophysiological or neuroimaging signals have varying degrees of signal-to-noise ratio (SNR), which will be briefly reviewed below.

- In vivo extracellular electrophysiology: Neuronal firing gives rise to transmembrane currents that are measured in the extracellular medium. Based on implanted multi-electrodes or microelectrodes in the brain, one can extract low frequency (<150 Hz) signals known as local field potentials (LFPs) as well as high frequency (>300 Hz) signals known as multi-unit activity. LFP measures extracellular currents reflecting summed dendritic postsynaptic potentials in thousands to millions of pyramidal cells in parallel alignment. In addition to postsynaptic currents, neuronal spikes are known to contribute to the LFP (Buzsaki et al., 2012): First, increased spiking activity generates a broad-frequency spectrum with a power distribution that depends on the composition of the active cell types. Second, both increased spike frequency and synchrony increase spectral power, particularly in the higher-frequency (>100 Hz) bands. Additionally, field potentials filtered at ultra high frequency (>300 Hz) contain both subthreshold and superthreshold spiking activity that can be used for neural decoding (Cao et al., 2020; Nason et al., 2020). Electrophysiological recordings are widely adopted in animal studies, and provides excellent cellular and temporal resolution.
- Neuroimaging: Functional magnetic resonance imaging (fMRI) and positron emission topography (PET) imaging are two most popular tools used in human pain studies (Morton et al., 2016). The blood-oxygen-level-dependent (BOLD) signal, detected in fMRI, reflects changes in deoxyhemoglobin driven by localized changes in brain blood flow and blood oxygenation, which are coupled to underlying neuronal activity by a process termed neurovascular coupling (Hillman, 2014). PET brain scan uses a radioactive substance called a tracer to show how the brain and its tissues are working. Unlike fMRI, PET incorporates the use of radiation. A review of pain neuroimaging in humans is referred to (Moayedi et al., 2018).
- Electroencephalography (EEG): Similar to the LFP, EEG measures extracellular currents but at a larger spatial scale that reflects the activity of hundreds of millions of

neurons. Despite the varying skull conductivity in the human head, the electrical field is powerful enough to be measured from EEG electrodes placed on the head. EEG can also measure the pain stimulus-evoked potentials (EPs) or event-related potentials (ERPs). Compared to fMRI or PET, EEG is appealing for its high temporal resolution, low cost, broad availability and ease of data collection.

- MEG: Both EEG and MEG measure the consequences of transmembrane currents (Buzsaki et al., 2012; Pesaran et al., 2018), but unlike EEG that measures potential differences that reflect volume currents across different locations on the scalp, MEG measures the extracranial magnetic fields predominantly related to primary dendritic currents or intracellular current flowing through dendrites that produce magnetic fields. As a consequence, the distortive effect of skull and skin compartments is smaller in MEG than in EEG outside of the head.
- Electrocorticogram (ECoG), also known as intracranial EEG, is referred to as the signal measured from macroelectrodes placed directly on the surface of cortex of epileptic patients (for the purpose of localization of the seizure focus). Unlike the noninvasive scalp EEG, intracranial EEG or ECoG is invasive, which measures the local brain signal (typically 2-3 mm in diameter) around the recording electrodes (Dubey and Ray, 2019). Similar to EEG, ECoG can measure pain-evoked potentials (Chen et al., 2007), with an improved SNR. In some studies, implanted electrodes can not only record neural signals from a specific site but also simultaneously stimulate the human brain at another area, providing information about the causal importance of a given brain area (Parvizi and Kastner, 2018).
- Optical calcium imaging of bulk-loaded fluorescent indicators can be used to record the spiking activity of hundreds or thousands of neurons. The fluorescence traces measures dynamic calcium flux within neurons and neuronal tissue. Calcium imaging has been used to investigate pain mechanisms in the spinal cord (Xu and Dong, 2019; Gao et al., 2021), and has been recently applied to the cortical-subcortical areas (Corder et al., 2000; Acuna et al., 2020; Li et al., 2021). Recent rapid advances in neurotechnology have provided faster, deeper, and more efficient neuronal readout from awake animals,

matching the traditional strengths of large-scale electrophysiology based on multielectrode arrays (Lecoq et al., 2019; Wei et al. 2020; Chen and Pesaran, 2021). New optical voltage imaging technologies can potentially improve the spatiotemporal resolution and SNR in optical imaging (Knöpfel and Song, 2019).

As pain results from the integration of nociceptive and contextual information mediated by both feedforward and feedback processes, multimodal brain recordings may provide researchers complementary views on the complex and dynamic brain activity during pain processing. In addition to brain signals, simultaneous measurements of physiological signals during pain experiments may include EMG, skin conductance, heart rate variability and cardiovascular reactivity.

3.3 Signal processing and feature selection

After neural data acquisition, the first-stage of neural data analysis is signal preprocessing. One of the tasks of preprocessing is to extract the signals of interest (e.g., spike sorting from extracellular recordings, source localization from EEG/MEG recordings), and another task is to suppress noise and improve the SNR (e.g., bandpass filtering and artifact rejection). The second stage of neural data analysis is feature extraction, with an aim to identify the most discriminative information for pain decoding. These two steps are important for the subsequent stages of pain decoding analyses.

Spike sorting Extracellular raw signals are recorded directly from the implanted microwires inside the brain. Signals are amplified, high-pass filtered (>300 Hz) and detected by an amplitude threshold. Features of the spike waveforms (such as the peak amplitude, energy, peak-to-trough width) are extracted and the spikes are subsequently sorted. Spikes with similar clustered features are grouped together into a single-unit, which yields neuronal spike activity. To date, state-of-the-art automated and scalable hardware-empowered spike sorting can accommodate real-time processing for large-scale data acquisition (Pachitariu et al., 2016; Chung et al., 2017; Jun et al., 2017; Yger et al., 2018)

Spike deconvolution for calcium imaging In optical calcium imaging, the Ca²⁺ dynamics are characterized by the fluorescence traces, which are typically shown in units of a percentage change of each imaged neuron's baseline fluorescence level. Upon preprocessing the raw signals, spike inference or spike deconvolution methods are required to estimate the calcium concentration and the spiking activity (proxy) (Pnevmatikakis et al., 2016; Friedrich et al., 2017; Pachitariu et al., 2018; Giovannucci et al., 2019). We use the term "proxy" because the relationship between fluorescence and spiking activity is rather complex and requires both forward and inverse modeling (Wei et al. 2020).

EEG artifact rejection and source localization Human EEG recordings are subject to various sources of independent noise and artifacts (such as eye blink, head movement, respiration). Extraction and removal of these components are usually done by independent component analysis (ICA) (Raduntz et al., 2015; Jas et al., 2017; Jiang et al., 2019).

The goal of EEG source localization is to estimate the location and strengths of the current sources ("dipole") that generate the multichannel EEG signals (similarly for MEG). Some constraints, such as the minimum norm or sparsity, are usually imposed. A standard tool for source localization is the minimum norm estimator (MNE). Given M-channel EEG signals, $\mathbf{Y} \in \mathbb{R}^{M \times T}$, the EEG time series with duration T is represented as a weighed sum of an ensemble of N dipoles plus additive background Gaussian noise

$$\mathbf{Y} = \mathbf{A}\mathbf{X} + \mathbf{V} = \sum_{n=1}^{N} \mathbf{A}_n \mathbf{X}_n + \mathbf{V}$$
 (1)

where $\mathbf{X} \in \mathbb{R}^{N \times T}$ contains the amplitudes of the unknown current dipole source, $\mathbf{A} \in \mathbb{R}^{M \times N}$ is a lead-field matrix governed by the quasi-static approximation of Maxwell's equations. In Eq. (1), the columns of $\mathbf{A} = \{A_n\}$ (where $A_n \in \mathbb{R}^{M \times 1}$) and rows of $\mathbf{X} = \{X_n\}$ (where $X_n \in \mathbb{R}^{1 \times T}$) are grouped together according to N ($N \gg M$) cortical surface patches. The noise covariance matrix for \mathbf{V} can be estimated from resting-state EEG data. The forward solution can be calculated using a three-compartment boundary-element model.

EEG channel selection and spatial patterns Finding meaningful EEG patterns from high-dimensional recording channels consists of dimensionality reduction (channel selection) and feature extraction (pattern optimization). For supervised discrimination, learning common EEG components that distinguish different task conditions or brain states is an effective feature extraction strategy for classification (Koles et al., 1990). The goal of common spatial pattern (CSP)-type algorithm is to find common EEG components with the largest variance ratios between two conditions (e.g., pain vs. no-pain). Given M-channel EEG signals (assuming zero mean for each channel), the optimization objective of CSP is to seek a set of linear transformation (spatial filters) that maximizes the ratio of the transformed data's variance between two conditions:

$$\max_{\mathbf{w}} J(\mathbf{w}) = \frac{\mathbf{w}^{\top} \mathbf{R}^{(1)} \mathbf{w}}{\mathbf{w}^{\top} \mathbf{R}^{(2)} \mathbf{w}} \quad \text{s.t.} \quad \|\mathbf{w}\|_{2} = 1$$
 (2)

where $\mathbf{w} \in \mathbb{R}^M$ denotes the spatial filter, and $\mathbf{R}^{(k)}$ denotes the sample spatial covariance matrix for the k-th condition (k = 1, 2). Maximization of the Rayleigh quotient $J(\mathbf{w})$ can be formulated as the solution to a generalized eigenvalue problem by simultaneous diagonalization of the covariance matrices $\mathbf{R}^{(1)}$ and $\mathbf{R}^{(2)}$. CSP is widely used in EEG spatio-spectral feature extraction, and has also been adapted for the analysis of ERP (Wu et al., 2013; Congedo et al., 2016). Probabilistic formulation of the CSP algorithm is discussed in (Wu et al., 2011; Wu et al., 2015; Wu et al., 2016).

Temporal and spectral patterns Pain is associated not only with a spatially extended network of dynamically recruited brain areas but also with complex temporal-spectral patterns of brain activity. Brain rhythms or neural oscillations are driven by fluctuations in excitability of populations of neurons, and have complex spatiotemporal patterns that vary in amplitude, timing, and frequency. Pain-induced brain rhythms include oscillatory activities at various frequency ranges (Ploner et al., 2017). Common spectral features include power spectral density, relative power (e.g., gamma to broadband power) ratio, amplitude and phase coherence, and phase synchrony; standard temporal features include ERP amplitude/latency, and phase amplitude coupling (PAC) (Xiao et al., 2019b).

Table 1: Brain oscillations in acute and chronic pain.

References	Neural oscillations	Brain area	Pain coding
(Gross et al., 2007; Hauck et al., 2007)	MEG gamma (60-95 Hz)	human S1, S2	acute pain perception
(Lim et al., 2016)	MEG theta, beta and gamma	human PFC, OFC, insular, S1, S2	fibromyalgia
(Kisler et al., 2020)	MEG theta, low gamma (31-60 Hz), alpha (8-13 Hz)	human S1, S2, insular	chronic neuropathic pain
(Zhang et al., 2007)	EEG gamma	human S1	subjective pain intensity
(Sarnthein et al., 2006)	EEG theta	human (all electrodes)	chronic neurogenic pain
(Stern et al., 2006)	EEG theta and low beta (12-16 Hz)	human insular, ACC, PFC, PPC, S1, S2	chronic neurogenic pain
(Gonzalez-Roldan et al. 2013)	EEG beta (16-30 Hz)	human insular, frontal lobe	fibromyalgia
(Schouppe et al., 2020)	EEG ERP	human somatosensory	subacute and chronic low back pain
(Green et al., 2009)	LFP spindle (8-14 Hz)	human sensory thalamus, PAG	subjective pain intensity, neuropathic pain
(Huang et al., 2016)	LFP theta, high beta	human sensory thalamus, PAG, PPVG	pain relief
(Malinen et al., 2010)	BOLD high-freq (0.12-0.25 Hz)	human insular, ACC	chronic pain
(Baliki et al., 2011)	BOLD high-freq (0.12-0.2 Hz)	human mPFC	chronic back pain
(Alshelh et al., 2016)	BOLD infra-slow (<0.1 Hz)	human dorsal horn, somatosensory thalamus	chronic neuropathic pain
(LeBlanc et al., 2014)	LFP theta	rat S1	acute and chronic pain
(LeBlanc et al., 2016)	EEG theta	rat S1, PFC	acute, inflammatory and neuropathic pain
(Wang et al. 2016)	ECoG gamma	rat S1	chronic inflammatory pain
(Zhang et al., 2018)	LFP theta, gamma	rat ACC	acute pain

A cortical ERP usually reflects the coordinated behavior of a large number of neurons in relation to an external stimulus. In EEG recordings, pain-evoked ERPs are commonly observed by trial averaging, whereas results of single-trial analyses are more highly variable (Chen et al., 2007). In the frequency domain, pain-evoked ERPs are accompanied with an increased theta band (4-8 Hz) power—known as the theta-event-related synchronization (ERS). In evoked pain, LFPs have shown an increased activity at the high-gamma band (60-100 Hz) (Zhang et al., 2018) as well as at the ultra-high frequency band (>300 Hz) (Sun et al., 2021b). These high-frequency LFP activity is mostly related to increased spiking activity at the population level. In chronic pain, over-relaxation in theta and beta bands have been observed (Sarnthein et al., 2006; Stern et al., 2006; Gonzalez-Roldan et al. 2013). For a review of brain rhythms of pain, see (Ploner et al., 2017; Pinheiro et al., 2016). Table 1 highlights some representative references in pain-induced brain oscillations from both human and animal research.

Connectivity and network patterns Functional connectivity (FC) of the brain describes the second-order pairwise statistics between large brain regions, and has been used in brain-wide neuroimaging based pain studies (Baliki et al., 2012; Necka et al., 2019; Vachon-Presseau et al., 2019; Kano et al., 2020; Spisak et al., 2020). For example, FC has been used to identify long-range nociceptive information flow within the brain in chronic pain conditions (Baliki et al., 2012; Necka et al., 2019; Vachon-Presseau et al., 2019). From LFP and EEG signals, directed FC or information flow can be computed based on frequency-domain Granger causality (Guo et al., 2020) or time-domain Granger prediction (Tøttrup et al., 2021). FC analyses can be generalized to population neurons based on calcium imaging

(Li et al., 2021).

On the other hand, network graph-theoretic measures are widely used to characterize internetwork connectivity within brain regions based on *in vivo* brain imaging data (Sporns et al., 2005; Bassett and Bullmore, 2006; Bullmore and Sporns, 2009). In the graph theory, betweenness centrality (CB) is a measure of the volume of shortest paths that pass through a given node (Kwon et al., 2019), which provides insight into the importance of that node (as a hub) in the passage of information throughout the network. Meanwhile, degree centrality (CD) is a measure of the number of edges attached to a given node (Kwon et al., 2019), which indicates its level of connectivity of this node as a functional hub to other nodes within the entire network. For a review, see (Vecchio et al., 2017).

4 A Review of Pain Decoding Methods

In this section, we will provide an overview of the state-of-the-art methods for pain decoding based on univariate or multivariate features derived from brain signals. The computational task of pain decoding analyses may include classification, prediction and detection, and risk assessment. We will cover both supervised and unsupervised ML approaches, as well as model-free and model-based approaches. The literature on this topic is growing rapidly, and by no means our review here is a complete coverage. A tabular list of representative references is summarized in Table 2.

4.1 Supervised learning

To decode pain, the most widely used ML methods in the literature is supervised learning. The basic idea is to identify spatial, temporal or spectral features from brain signals (fMRI, EEG or electrophysiology) and train the labeled data using parametric or nonparametric classifiers. Depending on the tasks, different ML tools are used for achieving specific goals.

- Predicting subjective pain level (e.g., scale 0-9)
- Detecting pain continuously
- Classifying pain vs. no pain from discrete episodes

- Classifying different pain intensities (e.g., low, medium and high-intensities)
- Classifying different pain experiences (e.g., physical vs. social pain)

The first task is a regression problem, the second task is a detection problem, and the remaining tasks are classification problems. For either regression or classification problem, supervised learning requires a large number of labeled samples. In practice, the number of labels are limited by the experimental conditions, such as the number of participants and the number of trials or sessions per condition.

Multivariate parametric classifiers The most common multivariate parametric analysis is driven by Fisher linear discriminant analysis (LDA), linear or generalized linear models (GLMs), including regularized LASSO (Least Absolute Shrinkage and Selection Operator) regression and logistic regression. Empirical Bayes (NB) is another popular classification method, as an approximation to a fully Bayesian treatment of a hierarchical Bayes model. The NB classifier assumes the features are conditionally independent given the class label. For the real-valued features, the Gaussian likelihood model is often assumed; for the binary features, the Bernoulli distribution model is assumed; whereas for the categorical features, the multinoulli distribution is assumed (Murphy, 2012).

Nonparametric classifiers Support vector machine (SVM) is a discriminative classifier that constructs the classification boundary by a separating hyperplane with maximum margin. Specifically, SVM maps the input into a high-dimensional feature space and maximizes the margin from the hyperplane to the origin. The nonlinear decision function can be written as follows

$$y(\mathbf{x}_i) = \operatorname{sgn}\left(\sum_{i=1}^n \alpha_i K(\mathbf{x}, \mathbf{x}_i) + b\right)$$

where $y_i \in \{-1, +1\}$ denotes the binary class label for the training sample \mathbf{x}_i ; $\alpha_i \geq 0$ is a sparse coefficient, and \mathbf{x}_i associated with $\alpha_i > 0$ are called support vectors; n denotes the training sample size; b denotes the bias, and $K(\cdot, \cdot)$ is a reproducing kernel function. Because of its powerful generalization, SVM classifiers are widely used in pain decoding

Table 2: A tabular survey of machine learning methods for detecting pain from brain signals.

References	Method	Data	Generalization	Acute or Chronic	Performance summary (no. subjects)	
(Brown et al., 2011)	SVM	human fMRI	Cross-subject	acute pain	81% accuracy (N = 24)	
(Brodersen et al., 2012)	SVM	human fMRI	Cross-subject	acute pain	62% accuracy (N = 16)	
(Schulz et al., 2012)	SVM	human EEG	Cross-subject	acute pain	83% accuracy ($N = 23$)	
(Huang et al., 2013)	NB classifier, SVM, LDA	human EEG	Cross-subject	acute pain	86.3% and $80.3%$ (within- and cross-subject) accuracy ($N=29$)	
(Wagner et al., 2013)	LASSO-PCR	human fMRI	Cross-subject	acute pain	>94% sensitivity and specificity (N = 20)	
			Cross-subject	social pain	85% sensitivity and 73% specificity ($N = 40$)	
(Vijayakumar et al., 2017)	RF	human EEG	Cross-subject	acute pain	89.45% accuracy (N = 25)	
(Lopez-Sola et al., 2017)	SVM	human fMRI	Cross-subject	fibromyalgia	92% sensitivity, 94% specificity ($N = 72$)	
(Kuo et al., 2017)	linear regression	human rs-MEG	Cross-subject	endogenous pain	0.64 correlation coefficient $(N=33)$	
(Lee et al., 2019)	SVM	human rs-fMRI	Cross-subject	chronic low back pain	92.5% accuracy, 0.97 AUC (N = 53)	
(Dinh et al., 2019)	SVM	human rs-EEG	Cross-subject	chronic pain	57% accuracy (N = 185)	
(Sun et al., 2021a)	SSM, SVM	human EEG	Cross-subject	acute pain	0.62-0.65 AUC (unsupervised), median 0.7 AUC (supervised) ($N = 32$)	
(Xiao et al., 2019a)	SSM	rat S1+ACC spikes	Cross-session	acute pain	71%-75% TP, 7-38% FP (same animal)	
(Sun et al., 2021b)	SSM	rat S1+ACC LFPs	Cross-session	acute, chronic pain	0.7-0.8 detection rate (same animal)	

applications (see Table 2).

The random forest (RF) is an ensemble learning method for classification or regression tasks by constructing many decisions trees (Hastie et al., 2008). It uses bagging and feature randomness when building each individual tree to create an uncorrelated forest of trees whose committee prediction is more accurate than that of any individual tree. RF uses two key concepts: (i) random sampling of training data points when building trees; and (ii) random subsets of features considered when splitting nodes. As a result, RF can well handle the overfitting problem even in the presence of large number of model parameters.

The Gaussian process (GP) classifier is a Bayesian nonparametric method used for binary classification. The key feature of GP is that the prediction is probabilistic so that one can compute empirical confidence intervals (Rasmussen and Williams, 2009). The GP classifier defines a smoother prior as a GP, which is characterized by a mean function and covariance function. The predictive posterior probability for each class is computed by integrating all unknown model hyperparameters.

Supervised learning methods have been widely used to decode pain based on human fMRI and EEG data (see Table 2). Figure 2 and Figure 3 present some illustrative examples on representative fMRI and EEG-based pain studies, respectively.

4.2 Unsupervised learning

In stochastic processes, change points are defined statistically by the meaning of "changes", such as the mean, variance, correlation, or spectral density. The observed uni- or multi-variate brain signal, as a form of spike trains, LFP or EEG time series, can be modeled as

a stochastic process. Therefore, proper statistical assumptions of the observed signals are required to formulate a change-point detection problem.

Model-free change-point detection One of the classic theories for change-point detection is the likelihood-ratio test, which computes the log-likelihood ratio (LLR) test statistic:

$$LLR = \max_{\tau} \{ \ell(z_{1:\tau}) + \ell(z_{\tau+1:n}) - \ell(z_{1:n}) \}.$$
 (3)

The log-likelihood (denoted by ℓ) of the statistical model including a change will provide an improvement over the model with no change. Therefore, a change-point is inferred if LLR > θ_0 for a preselected threshold θ_0 . If a change-point is inferred, then its detection latency is estimated as

$$\tau = \arg\max\{\ell(z_{1:\tau}) + \ell(z_{\tau+1:n}) - \ell(z_{1:n})\}. \tag{4}$$

Detection is faced with the trade-off of speed and accuracy, whereas change-point detection aims to achieve quickest detection while maintaining good accuracy. For acute pain, the detection latency is defined as the time it takes to detect pain signal (according to a predefined statistical criterion) from the stimulus onset. The detection time may occur sooner or later than the onset of subject's reaction time or animal's paw withdrawal (i.e., reflexive pain behavior).

The CUSUM (cumulative sum) algorithm is a classic model-free method for changepoint detection, and has been used in neuroscience applications (Koepcke et al., 2016). A modified CUSUM algorithm has been developed for detecting changes in single or multiunit spiking activity, which is assumed to be drawn from a homogeneous Poisson process (Chen et al., 2017a). Given two Poisson distributions f_1 and f_0 , let's assume that their rate parameters are λ_1 , and λ_0 , respectively. The LLR between these two Poisson distributions is given as $\log \frac{f_1}{f_0} = y \log \frac{\lambda_1}{\lambda_0} - (\lambda_1 - \lambda_0)$. Let us further assume that the baseline rate λ_0 is known or can be estimated directly from data. Since the Poisson variance is equal to the mean, a statistical criterion for a significant increase in λ_1 is set as: $\lambda_1^{\text{significant}} = \lambda_0 + 2\sqrt{\lambda_0} \geq 0$. In this case, the LLR is given as (Chen et al., 2017a)

$$LLR_{f_1 \parallel f_0} = y \log \frac{\lambda_1^{\text{significant}}}{\lambda_0} - (\lambda_1^{\text{significant}} - \lambda_0)$$
 (5)

Given the initial $S_0 = 0$, the cumulative sum of LLR is updated as follows

$$S_k = \max_{c=1,\dots,C} \left\{ S_{c,k} \right\} = \max_{c} \left\{ \max \left\{ 0, S_{c,k-1} + s_{c,k} \right\} \right\}$$

where $s_{c,k}$ is computed from the LLR (Eq. 5) using $y_{c,k}$ from the c-th neuron. If the cumulative sum of the statistic S_k is above a predetermined threshold θ_0 and the trend continues more than two or three steps, then a change point is determined and S_k is reset. The threshold θ_0 in the CUSUM algorithm controls the false alarm rate, which can be set using the test statistic (twofold log-likelihood) of a chi-square distribution with 1 degree of freedom: $\chi^2_{1,(1-\alpha)}$; if $\alpha = 0.01$, then the threshold is $\theta_0 = 3.38$.

State space model (SSM)-based change-point detection Pain perception is a dynamic process, and the pain percept can be modeled as a latent variable. The problem of detecting the onset of pain signals can be formulated as a change-point detection problem and resolved by state-space analysis (Chen et al., 2017a; Chen et al., 2017b; Hu et al. 2017; Hu et al., 2018). The SSM consists of a state equation and a measurement equation (Chen, 2015). In the state equation, the multivariate neural activity $\mathbf{y}_k = [y_{1,k}, \dots, y_{C,k}]^{\top}$ at time k, represented by a C-dimensional vector, is assumed to be driven by a common univariate latent Markovian process z_k :

$$z_k = az_{k-1} + \epsilon_k \tag{6}$$

where $\epsilon_k \in \mathcal{N}(0, \sigma_{\epsilon}^2)$ specifies a temporal Gaussian prior (with zero mean and variance σ_{ϵ}^2) on the latent process that describes a first-order autoregressive (AR) model, and 0 < |a| < 1 denotes the AR coefficient. The measurement equation characterizes the likelihood model for the observed brain signals. In the case of spike count observations from neuronal ensembles, we can use a generative model known as Poisson linear dynamical system (PLDS)

(Chen et al., 2017a):

$$\eta_k = \mathbf{c}z_k + \mathbf{d} \tag{7}$$

$$\mathbf{y}_k \sim \operatorname{Poisson}\!\left(\exp(\boldsymbol{\eta}_k)\Delta\right)$$
 (8)

where Δ denotes the temporal bin size, and \mathbf{y}_k denotes the spike count drawn from a timevarying inhomogeneous Poisson process with rate η_k . Here, the parameters \mathbf{c} and \mathbf{d} are unconstrained in the PLDS model.

Alternatively, the spike count vector can be transformed using the change-of-variable, such as $\tilde{\mathbf{y}}_k = \sqrt{\mathbf{y}_k}$ or $\tilde{\mathbf{y}}_k = \log(\mathbf{y}_k + 1)$. Assuming that the transformed variable $\tilde{\mathbf{y}}_k$ is Gaussian, one can use the transformed linear dynamical system (TLDS) (Chen et al., 2017b):

$$\tilde{\mathbf{y}}_k = \mathbf{c}z_k + \mathbf{d} + \mathbf{w}_k \tag{9}$$

where $\mathbf{w}_k \in \mathcal{N}(\mathbf{0}, \mathbf{\Sigma}_{\mathbf{w}})$ is a Gaussian noise process with zero mean and covariance $\mathbf{\Sigma}_{\mathbf{w}}$. The same modeling and analysis of TLDS can be generalized to continuous-valued measurements, such as LFP or EEG-derived power or amplitude features (Sun et al., 2021a; Sun et al., 2021b).

For both PLDS and TLDS models, a likelihood approach is used to estimate the unknown state variables $z_{1:T}$ and parameters $\Theta = \{a, \mathbf{c}, \mathbf{d}, \sigma_{\epsilon}\}$ or $\Theta = \{a, \mathbf{c}, \mathbf{d}, \Sigma_{\mathbf{w}}\}$ from a set of observations $\mathbf{y}_{1:T}$. The joint state and parameter estimation can be tackled by the expectation-maximization (EM) algorithm (Macke et al., 2015). The EM algorithm has a closed-form solution for TLDS; whereas in the case of PLDS, an approximate EM algorithm can be derived. In the E-step, a forward-backward Kalman smoother is run based on variational or Laplacian approximation of the Poisson likelihood, from which the Gaussian sufficient statistics of latent state are derived: $\mathcal{N}(\hat{z}_{k|T}, Q_{k|T})$. In the M-step, the likelihood function is optimized with respect to the unknown parameters. The baseline parameter \mathbf{c} can be set by the sample statistics. Additionally, the parameters a, \mathbf{d} and σ_{ϵ}^2 can be derived with the closed-form solutions (Macke et al., 2015; Chen, 2015;

Table 3: Online recursive filtering for estimating the latent variable z_k in the PLDS and TLDS models $(Q_{k|k} = \text{Var}[\hat{z}_{k|k}]$ denotes the filtered state variance).

	PLDS	TLDS			
Prediction	$\hat{z}_{k k-1} = a\hat{z}_{k-1 k-1}$				
equations	$Q_{k k-1} = a^2 Q_{k-1 k-1} + \sigma_{\epsilon}^2$				
Update	$\hat{\mathbf{y}}_{k k-1} = \exp(\mathbf{c}\hat{z}_{k k-1} + \mathbf{d})\Delta$	$\hat{\mathbf{y}}_{k k-1} = \mathbf{c}\hat{z}_{k k-1} + \mathbf{d}$			
equations	$Q_{k k}^{-1} = Q_{k k-1}^{-1} + \mathbf{c}^{T} diag(\hat{\mathbf{y}}_{k k-1})\mathbf{c}$	$\mathbf{G}_k = Q_{k k-1} \mathbf{c}^{T} (Q_{k k-1} \mathbf{c} \mathbf{c}^{T} + \Sigma_{\mathbf{w}})^{-1}$			
	$\hat{z}_{k k} = \hat{z}_{k k-1} + Q_{k k} \mathbf{c}^{\top} (\mathbf{y}_k - \hat{\mathbf{y}}_{k k-1})$	$\hat{z}_{k k} = \hat{z}_{k k-1} + \mathbf{G}_k(\mathbf{y}_k - \hat{\mathbf{y}}_{k k-1})$			
		$Q_{k k}^{-1} = Q_{k k-1}^{-1}(1 - \mathbf{G}_k \mathbf{c})$			

Chen, 2021). The E- and M-steps are executed alternatively and iteratively until the loglikelihood reaches a local maximum.

Once the model parameters are identified, a forward recursive filter is used to estimate the latent state variable for either PLDS or TLDS model (Table 3). In a standard setting, Gaussian process noise is assumed in the state equation (Eq. 6). To further improve the detection speed, non-Gaussian dynamical noise can be introduced for modeling a stochastic jump process in the latent state dynamics (Chen, 2003; Doucet et al., 2000). Accordingly, particle filtering and smoothing algorithms can be developed for accommodating non-Gaussian noise and non-Gaussian likelihood (Hu et al., 2018).

Given an online estimation of latent variable $\hat{z}_{k|k}$ at time step k, a Z-score statistic (for measuring the relative change) is computed with respect to the baseline: Z-score = $\frac{\hat{z}_{k|k}-\text{mean of }z_{\text{baseline}}}{\text{SD of }z_{\text{baseline}}}$, which also yields a probability of change (Chen et al., 2017b):

Prob{Z-score
$$> \theta_0$$
} = $1 - \int_{-\infty}^{\theta_0} \frac{1}{\sqrt{2\pi}} e^{\frac{-u^2}{2}} du$ (10)

The criterion of Z-score change is determined by a statistical threshold θ_0 depending on the significance level. When P = 0.05, $\theta_0 = 1.65$; when P = 0.01, $\theta_0 = 2.33$; when P = 0.001, $\theta_0 = 3.08$. Therefore, it is inferred that a change-point occurs when Z-score – CI > θ_0 or Z-score + CI < $-\theta_0$, where the CI denotes the confidence interval (CI) derived from the posterior variance of $\hat{z}_{k|k}$. Note that the algebraic sign of the Z-score is irrelevant due to the algebraic sign ambiguity of $\{\hat{z}_{k|k}\}$ in model estimation.

The SSM method for detection of acute pain signals can be applied to spiking, EEG and LFP data (Chen et al., 2017a; Hu et al., 2018; Sun et al., 2021a; Sun et al., 2021b).

See Fig. 4 for some illustrative examples.

Multi-region and multi-modal decoding In the presence of using detectors for multiple brain regions (ACC and S1), different modalities (spikes vs. LFP), or different models (PLDS vs. TLDS), a rule is required to integrate the decisions from multiple detectors.

In the case of two simultaneously recorded brain regions, a cross-correlation function (CCF) can be computed to correlate the two Z-scores derived from the ACC and S1 recordings (spikes or LFPs). Specifically, let $\{Z_k^{\text{ACC}}\}$ and $\{Z_k^{\text{S1}}\}$ denote the derived Z-scores from the ACC and S1 signals, respectively, the moving-average CCF between two Z-scores are defined as (Xiao et al., 2019a)

$$CCF_k = (1 - \rho)CCF_{k-1} + \rho(Z_k^{ACC})^m (Z_k^{S1})^n$$

where $0 < \rho < 1$ is a forgetting factor, $0.5 \le m, n \le 1$ are the scaling exponents (default value: 0.5). The smaller the forgetting factor ρ , the smoother becomes the CCF curve. A smaller exponent value will magnify the impact of Z-score smaller than 1, while reducing the impact of a higher Z-score. When two Z-score traces follow a consistent trend, the CCF will increase in absolute value, and stay at the baseline level otherwise. To track the significant change, we can compute the CCF area above the threefold SD of baseline statistics, and determine change points when the accumulated area value exceeds a predefined threshold (Xiao et al., 2019a).

In the case of simultaneously recorded spikes and LFP, we can assume that these two modalities are conditionally independent and derive the joint likelihood

$$P(\mathbf{y}_k^{\text{spike}}, \mathbf{y}_k^{\text{LFP}}|z_k) = P(\mathbf{y}_k^{\text{spike}}|z_k)P(\mathbf{y}_k^{\text{LFP}}|z_k)$$

where z_k denotes the latent variable representing the pain signal. The spike and LFP likelihood functions can be characterized by Poisson and Gaussian models, respectively. A modified EM algorithm can be derived for the SSM with mixed modalities.

Furthermore, it is possible to generalize the setting to more than two regions, each with multiple modalities. In that case, we would potentially have N independent predictors re-

sulted from different combinations. A final decision needs to be reached based on ensemble's prediction using different voting strategies: (i) Hard voting or majority vote: predicting the class with the largest sum of votes from individual predictors. (ii) Soft or weighted voting: predicting the class with largest summed probability from individual predictors. The weight from each predictor may be equal or non-equal according to their relative importance; and the averaging can be based on either arithmetic mean or geometric mean.

4.3 Comparison between supervised and unsupervised learning methods

Supervised learning methods rely on the availability of labeled samples. This can be challenging in some pain experiments because of the ethical consideration. As result, overfitting is a concern for generalization. Therefore, regularization and feature extraction are important to alleviate overfitting. Another concern in the classification problem is sample imbalance between positive and negative classes. A classification dataset with skewed class proportions is called an imbalanced dataset (He and Garcia, 2009). Classes that make up a larger (or smaller) proportion of the dataset are called majority (or minority) classes. One way to handle imbalanced data is undersampling, which aims to downsample and upweight the majority class. The other way is to oversampling, which is the process of randomly duplicating observations from the minority class in order to reinforce its signal. The SMOTE (Synthetic Minority Over-sampling Technique) (Chawla et al., 2002) and ADASYN (Adaptive Synthetic Sampling) algorithms (He et al., 2008) are commonly used for oversampling.

In contrast, unsupervised learning methods can alleviate the need of large labeled samples, and has been demonstrated to have good generalization for across-trial, across-session, across-stimulation, and across-subject conditions (Hu et al., 2018; Xiao et al., 2019a; Sun et al., 2021a; Sun et al., 2021b). When the sample size is small, unsupervised learning will be more appealing. Combining the strengths of these two methods may be crucial for future pain decoding research.

Table 4: A list of representative human chronic pain studies.

References	Type of chronic pain	Data	# Subjects	Features
(Chiapparini et al., 2009)	chronic migraine	rs-fMRI	24	FC
(Burgmer et al., 2009)	fibromyalgia, tonic pain	task and rs-fMRI	27	FC
(Malinen et al., 2010)	chronic pain	rs-fMRI	20	FC
(Baliki et al., 2006)	chronic back pain	rs-fMRI	24	FC
(Baliki et al., 2012)	persistent subacute back pain	rs-fMRI	56	FC
(Barroso et al., 2021)	chronic osteoarthritis pain	rs-fMRI	114	FC
(Lee et al., 2019)	chronic low back pain	rs-fMRI	53	multimodal (CBF, FC, HRV)
(Dinh et al., 2019)	chronic back pain, chronic widespread pain	rs-EEG	185	FC

5 Challenges and Future Directions

5.1 Improving decoding accuracy

Deciphering brain signals has multiple bottlenecks, including the limited number of training samples, limited sampling (e.g., unit yield, channel count), neural plasticity and adaptation during the course of pain experiments. As a result, decoding pain from brain activity is subject to errors: false positives (FPs) and false negatives (FNs). One reason for FPs is because even pain-responsive areas do not exclusively respond to pain. Therefore, additional recordings of brain signals from other non-pain-modulated regions (such as the visual cortex or motor cortex) can help reduce or eliminate the false positive. In addition, it is important to distinguish the difference between decoding pain and decoding saliency or pain anticipation (Lee et al., 2020). For instance, ERPs may be induced by stimulus saliency instead of pain (Iannetti et al., 2008; Iannetti et al., 2013). One reason for FNs is the relative contribution of individual pain-modulated regions may be unequal, which may depend on the condition or subcategory of pain. Determining the weights of independent "weak" decoders to form an ensemble pain decoding strategy may help reduce the FN rate.

Recently, convolutional neural networks (CNNs) and recurrent neural networks (RNNs) have been adopted to learn multichannel multichannel EEG spatiotemporal features (Gallagher et al., 2017; Bashivan et al., 2016; Stober et al., 2016). However, all deep learning methods have a large number of unknown parameters and require substantial labeled samples in training. Development of parameterized and interpretable deep learning models can help understand the learned spatial, temporal, and spectral features of the EEG (Li et al., 2017).

In parallel to brain signals, decoding pain can also benefit from combination of brain

activity with other non-neural modalities (Lancaster et al., 2017; Lee et al., 2019). To date, ML methods have been developed to decode pain based on facial expression (Prkachin et al., 1994; Blais et al., 2008; Chen et al., 2018; Dolenske et al., 2020) and facial movement (Bartlett et al., 2014).

5.2 Neurobiomarkers of chronic pain and acute-to-chronic pain transition

In comparison to acute or evoked pain, decoding tonic or spontaneous pain is more difficult, since the latter is not associated with external stimulus, and the neural signatures of spontaneous pain is still poorly understood. More importantly, successful prediction of pain does not imply that the predictive brain feature is specific to the experience of pain (Davis et al., 2017). From a clinical viewpoint, a biomarker is a biological measure of the presence or progress of a disease state. Identification of neurobiomarkers of chronic pain would help doctors assess and diagnose chronic pain patients, and monitor their responses to drug treatment (Davis et al. 2020). However, a neural signature of chronic pain that is consistently present across different types of pain has been elusive, partly due to the complexities and heterogeneity of chronic pain conditions (Kisler et al., 2020). Accordingly, the functional brain signatures may very likely be different for migraines, fibromyalgia, musculoskeletal pain, and chronic back pain (e.g., Table 4). Chronic pain also affects mental health, and has a negative impact on stress and depression. The brain activity of chronic pain patients may be confounded by underlying neuropsychiatric comorbidities. Therefore, large-scale longitudinal resting-state and task-based brain imaging from a large population cohort is required for a conclusive study on chronic pain. For detailed reviews on neuroimaging for chronic pain, see (Borsook et al., 2011a; Borsook et al., 2011b; Woo et al., 2017; Davis et al., 2017; Mouraux and Iannetti, 2018; van der Miesen et al., 2019). Compared to fMRI and PET, EEG has several significant advantages: high temporal resolution, portability and ease of operation in clinical setting. ML-empower neuroimaging approach can play a pivotal role in future neurobiomarker discovery and brain state classification (Wu et al., 2016; Reckziegel et al., 2019). Finally, there are only a few systematic investigations on predicting the transition from acute to chronic pain (Baliki et al., 2012). Because the temporal boundaries of the transition state remain unclear, and clinically this window is often even

inaccessible (patients are defined in acute pain or in chronic pain, but rarely in the transition phase), little knowledge is available regarding the underlying processes.

5.3 Brain machine interfaces for pain

Brain-machine interfaces (BMIs) are widely used in therapeutic applications to restore or enhance brain functions (Mickle et al., 2019; Grosenick et al., 2015; Andersen et al., 2019; Shanechi, 2019). Generally, the BMI has a signal detection/decoding arm and a feedback-driven control/modulation arm. Therefore, a closed-loop BMI system is ideally suited to demand-based pain management by selectively targeting discrete symptomatic episodes, especially during chronic pain conditions (Shirvalkar et al., 2018).

In a recent study, Zhang and colleagues (Zhang et al., 2020) examined healthy subjects receiving intermittent pain stimuli in a real-time fMRI-based closed-loop feedback-stimulation task, and showed that multi-voxel brain activity pattern decoding of pain intensity could be used to train a control algorithm to learn to deliver less painful stimuli (Fig. 5A). Specifically, they developed an ML-based decoder to investigate whether brain activity measured with fMRI and EEG could be used to predict pain in real-time, and showed how regionally and computationally specific co-adaptive brain-machine learning influenced the efficacy of closed-loop systems for pain.

As EEG is more convenient and cost effective than fMRI in human pain experiments, with the help of real-time source localization (Guarnieri et al., 2021), high-density EEG recordings are more ideal for the closed-loop human BMI system Recently, Tayeb and colleagues (Tayeb et al., 2020) identified a spatio-temporal EEG signature of brain activity during various degrees (innocuous, moderately more intense, and noxious) of stimulation of an amputee's phantom limb using transcutaneous electrical nerve stimulation (TENS). Based on the spatio-temporal EEG features, they developed a real-time BMI system to detect pain perception and classified three different stimulation conditions with a test accuracy of 94.66% (Fig. 5B). Based on EEG source localization, they found early strong ACC activation corresponding to the noxious stimulus condition, and activation of the posterior cingulate cortex (PCC) during the noxious sensation. The pain BMI system can provide therapeutic applications by neuromodulation. To date, neuromodulation for chronic pain

patients include spinal cord stimulation (SCS), percutaneous peripheral nerve stimulation (PNS), TENS, repetitive transcranial magnetic stimulation (rTMS), deep brain stimulation (DBS) and mortor cortex stimulation (MCS). A review of these neuromodulation technologies is referred to (Knotkova et al., 2021).

In animal studies, integration of electrophysiology and optogenetics provides a powerful platform to causally mapping cortical pain pathways in sensory or affective pain processing (Lee et al., 2015; Dale et al., 2018; Singh et al., 2020). Closed-loop rodent BMIs can causally perturb neural circuits and examine the change in brain signals and pain behavior at a millisecond temporal resolution (Zhang et al., 2021) (Fig. 5C). To translate this technology to a clinical setting, optogenetic stimulation in the modulation arm of the BMI can be replaced with electrical DBS (Zhou et al., 2019; Sun et al., 2021b; Gopalakrishnan et al., 2018). Additionally, LFP signals are more stable than neuronal spiking activity and are conceptually similar to ECoG or EEG signals. Combination of LFP pain detection and non-invasive brain stimulation techniques (e.g., ultrasound stimulation and transcranial electrical stimulation) will further advance the clinical application of closed-loop pain control in the future.

5.4 Future directions

Accumulated human and animal pain studies and neural recordings have continued to provide us valuable information about brain circuits and pain processing. Despite the rapid growth of neuroimaging and electrophysiological data, it remains difficult to draw a consensus or reconcile conflicting findings due to the differences in task design or experimental setup. It is also worth noting the fundamental limits of "decodability" of brain signals, for either fMRI (Jabakhanji et al., 2020) or EEG (Parvizi and Kastner, 2018). Because of potential overfitting, supervised decoding results based on a small sample size (< 100) should be especially cautioned with their result interpretability and generalizability (Varoquaux, 2018; Poldrack et al., 2020). Finally, we outline several important research directions in pain decoding that may help improve some of mentioned issues reviewed in the current paper.

First, EEG-based pain decoding would benefit from information collection from both cortical and subcortical areas. However, precise EEG localization of subcortical or deep brain activity remains challenging even with high-density EEG recordings (Seeber et al., 2014; Hnazaee et al., 2020). Advanced deep learning methods and new localization strategies may potentially improve the spatiotemporal resolution through data synthesis (Hecker et al., 2007; Huang et al., 2021; Wei et al. 2021).

Second, decoding pain, especially in chronic pain patients, shall consider available clinical and demographic data (e.g., gender, age, disease history, etc). As expected, ML algorithms for multimodal data-fusion can potentially help improve the diagnosis accuracy.

Third, it is critical for the pain research community to establish a public benchmark repository that accommodates high-quality electrophysiological and neuroimaging datasets, including multisite electrophysiological recordings from freely behaving animals, or simultaneous EEG-fMRI recordings from humans. Like any other research areas in ML, benchmark datasets will provide a means to compare different ML methods in classification or prediction tasks. Ideally, such datasets will include multiple independent recording sessions that allow within-subject and between-subject prediction.

References

Acuna MA, Kasanetz F, De Luna P, Nevian T (2020). Cortical representation of pain by stable dedicated neurons and dynamic ensembles. https://doi.org/10.1101/2020.11.02.364778

Alshelh Z, Di Pietro F, Youssef AM et al. (2016) Chronic neuropathic pain: it's about the rhythm. J. Neurosci. 36: 1008-1018.

Andersen RA, Aflalo T, Kellis S (2019). From thought to action: the brain-machine interface in posterior parietal cortex. Proc. Nat. Acad. Sci. USA 116: 26274-26279.

Apkarian AV, Bushnell MC, Treede R-D, Zubieta J-K. (2005). Human brain mechanisms of pain perception and regulation in health and disease. Eur. J. Pain 9: 463-484.

Babiloni C, et al. (2008). Cortical alpha rhythms are related to the anticipation of sensorimotor interaction between painful stimuli and movement: a high-resolution EEG study. J. Pain 9: 902-911.

Bagarinao, E. et al. (2014) Preliminary structural MRI based brain classification of chronic pelvic pain: a MAPP network study. Pain 155: 2502-2509.

Baliki MN, Chialvo DR, Geha PY, et al. (2011) Chronic pain and the emotional brain: specific brain activity associated with spontaneous fluctuations of intensity of chronic back pain. J. Neurosci. 26: 12165-12173.

Baliki MN, Baria AT, Apkarian AV (2011) The cortical rhythms of chronic back pain. J. Neurosci. 31: 13981-13990.

Baliki, M.N., Petre, B., Torbey, S., Herrmann, K.M., Huang, L., Schnitzer, T.J., Fields, H.L., Apkarian, A.V. (2012). Corticostriatal functional connectivity predicts transition to chronic back pain. Nat. Neurosci. 15: 1117-1119.

Bartlett MS, Littlewort GC, Frank MG, Lee K (2014) Automatic decoding of facial movements reveals deceptive pain expressions. Curr. Biol. 24: 738-743.

Barroso J, Wakaizumi K, Reis AM et al. (2021) Reorganization of functional brain network architecture in chronic osteoarthritis pain. Human Brain Mapp. 42: 1206-1222.

Bashivan P, Rish I, Yeasin M, Codella N (2016). Learning representations from EEG with deep recurrent-convolutional neural networks. Proc. Inter. Conf. learned Representations (ICLR'16). https://arxiv.org/abs/1511.06448

Bassett DS, Bullmore E (2006). Small-world brain networks. Neuroscientist 12: 512-523.

Besson JM (1999) The neurobiology of pain. Lancet, 353: 1610-1615.

Blais C, Fiset D, Furumoto-Deshaies H, Kunz M, Seuss D, Cormier S (2019) Facial features underlying the decoding of pain expressions. J Pain. 20:728-738.

Boonstra AM, Preuper HRS, Reneman MF, et al. (2008) Reliability and validity of the visual analogue scale for disability in patients with chronic musculoskeletal pain. International Journal of Rehabilitation Research, 31: 165-169.

Borsook, D., Becerra, L., Hargreaves, R. (2011a) Biomarkers for chronic pain and analgesia. Part 1: the need, reality, challenges, and solutions. Discov. Med. 11: 197-207.

Borsook, D., Becerra, L., Hargreaves, R. (2011b) Biomarkers for chronic pain and analgesia. Part 2: how, where, and what to look for using functional imaging. Discov. Med. 11: 209-219.

Brodersen KH, Wiech K, Lomakina EI, Lin CS et al. (2012) Decoding the perception of pain from fMRI using multivariate pattern analysis. Neuroimage 63: 1162-1170.

Brown, J. E., Chatterjee, N., Younger, J., Mackey, S. (2011) Towards a physiology-based measure of pain: patterns of human brain activity distinguish painful from non-painful thermal stimulation. PLoS ONE 6: e24124.

Bullmore E, Sporns O (2009). Complex brain networks: graph theoretical analysis of structural and functional systems. Nature Rev. Neurosci. 10: 186-198.

Burgmer M, Pogatzki-Zahn E, Gaubitz M, Wessoleck E, Heuft G, Pfleiderer B (2009). Altered brain activity during pain processing in fibromyalgia. Neuroimage. 44:502-508.

Bushnell MC, Ceko M, Low LA (2013) Cognitive and emotional control of pain and its disruption in chronic pain, Nat. Rev. Neurosci. 14, 502–511

Buzsaki G, Anastassiou CA, Koch C (2012). The origin of extracellular fields and currents-EEG, ECoG, LFP and spikes, Nat. Rev. Neurosci. 13, 407–420

Cao L, Varga V, Chen Z (2020). Spatiotemporal patterns of rodent hippocampal field potentials uncover spatial representations. Cell Rep. Methods, under revision. https://www.biorxiv.org/content/10.1101/828467v2

Chawla NV, Bowyer KW, Hall LO, Kegelmeyer WP (2002). SMOTE: synthetic minority over-sampling technique. Journal of Artificial Intelligence Research 16: 321-357.

Chen Z (2003). Bayesian filtering: From Kalman filters to particle filters, and beyond. Technical report, McMaster University.

Chen Z, editor (2015). Advanced State Space Methods for Neural and Clinical Data. Cambridge Univ. Press.

Chen Z, Ohara S, Cao J, Vialatte F, Lenz FA, Cichocki A (2007). Statistical modelling and analysis of laser-evoked potentials of electrocorticogram recordings from awake humans. Computational Intelligence and Neuroscience, Online Article ID 10479.

Chen Z, Hu S, Zhang Q, Wang J (2017a). Quickest detection for abrupt changes in neural ensemble spiking activity using model-based and model-free approaches. Proc. IEEE EMBS Neural Engineering Conference (NER), pp. 481-484.

Chen Z, Zhang Q, Tong APS, Manders TR, Wang J (2017b). Deciphering neuronal population codes for acute thermal pain. J. Neural Eng. 14: 036023.

Chen Z, Pesaran B (2021). Improving scalability in systems neuroscience. Neuron 109: 1776-1790.

Chen Z (2021). Real-time detection of acute pain signals based on spikes/LFP. In Thakor N. (editor) Handbook of Neuroengineering, Springer.

Chen Z, Ansari R, Wilkie DJ (2018) Automated pain detection from facial expressions using FACS: a review. https://arxiv.org/pdf/1811.07988.pdf

Cheppudira, B. P. (2006). Characterization of hind paw licking and lifting to noxious radiant heat in the rat with and without chronic inflammation. J. Neurosci. Methods 155: 122-125.

Chiapparini L, Grazzi L, Mandelli ML, et al. (2009) Functional-MRI evaluation of pain processing in chronic migraine with medication overuse. Neurological Sciences, 30: 71-74.

Chung JE, Magland JF, Barnett AH, et al. (2017). A fully automated approach to spike sorting. Neuron 95, 1381-1394.

Coghill RC, Sang CN, Maisog JM, Iadarola MJ (1999) Pain intensity processing within the human brain: a bilateral, distributed mechanism. J. Neurophysiol. 82: 1934-1943.

Cohen SP, Vase L, Hooten WM (2021). Chronic pain: an update on burden, best practices, and new advances. Lancet, 397: 2082-2097.

Congedo M, Korczowski L, Delorme A, da Silva FL (2016) Spatio-temporal common pattern: A companion method for ERP analysis in the time domain. Journal of Neuroscience Methods, 267: 74-88.

Corder G, Ahanonu B, Grewe BF, et al. (2019). An amygdalar neural ensemble that encodes the unpleasantness of pain. Science 363: 276-281.

Dale AM, et al. (2000). Dynamic statistical parametric mapping: combining fMRI and MEG for high-resolution imaging of cortical activity. Neuron 26: 55-67.

Dale J, Zhou H, Zhang Q, et al. (2018). Scaling up cortical control to inhibit chronic pain, Cell Rep. 23, 1301–1313.

Davis KD, Flor H, Greely, HT, et al. (2017). Brain imaging tests for chronic pain: medical, legal and ethical issues and recommendations, Nat. Rev. Neurology, 13: 624–638.

Davis KD, Aghaeepour N, Ahn AH, et al. (2020). Discovery and validation of biomarkers to aid the development of safe and effective pain therapeutics: challenges and opportunities. Nat. Rev. Neurol. 16: 381-400.

Desikan RS, et al. (2006). An automated labeling system for subdividing the human cerebral cortex on MRI scans into gyral based regions of interest. Neuroimage 31: 968-980.

Deuis, J. R., Dvorakova, L. S., and Vetter, I. (2017). Methods used to evaluate pain behaviors in rodents. Front. Molecular Neurosci. 10: 284.

Dinh ST, Nickel MM, Tiemann L, et al. (2019) Brain dysfunction in chronic pain patients assessed by resting-state electroencephalography. Pain, 160: 2751-2765.

Dolensek, N., Gehrlach, D. A., Klein, A. S. Gogolla, N. (2020). Facial expressions of emotion states and their neuronal correlates in mice. Science, 368: 89-94.

Doucet A, Godsill S, Andrieu C (2000) On sequential Monte Carlo sampling methods for Bayesian filtering. Statist. Comput. 10: 197–208

Downar J, Mikulis DJ, Davis KD (2003). Neural correlates of the prolonged salience of painful stimulation. Neuroimage 20: 1540-1551.

Dubey A, Ray S (2019) Cortical electrocorticogram (ECoG) is a local signal. J. Neurosci. 39: 4299-4311.

Fitzcharles MA, Cohen SP, Clauw DJ, Littlejohn G, Usui C, Huser W (2021). Nociplastic pain: towards an understanding of prevalent pain conditions. Lancet, 397: 2098-2110.

Fordyce WE, Lansky D, Calsyn DA, et al. (1984) Pain measurement and pain behavior. Pain, 18: 53-69.

Friedrich, J., Zhou, P., and Paninski, L. (2017). Fast online deconvolution of calcium imaging data. PLoS Computational Biology 13: e1005423. Friedrich J, Yang W, Soudry D, Mu Y, Ahrens MB, Yuste R, Peterka DS, Paninski L (2017). Multi-scale approaches for high-speed imaging and analysis of large neural populations. PLoS Comp. Biol. 13: e1005685.

Gallagher N, Ulrich KR, Talbot A, Dzirasa K, Carin L, Carlson DE (2017). Cross-spectral factor analysis. Advances in Neural Information Processing Systems 30, pp. 6845-6855.

Gao X, Han S, Huang Q, et al (2019). Calcium imaging in population of dorsal root ganglion neurons unravels novel mechanisms of visceral pain sensitization and referred somatic hypersensitivity. Pain, 162: 1068-1081.

Giovannucci A, Friedrich J, Gunn P, et al (2019). CaImAn an open source tool for scalable calcium imaging data analysis. eLife, 8: e38173.

Gonzalez-Roldan AM, Cifre I, Sitges C, Montoya P (2016) Altered dynamic of EEG oscillations in fibromyalgia patients at rest. Pain Med. 17:1058-1068.

Gopalakrishnan R, Burgess RC, Malone DA, et al. (2018). Deep brain stimulation of the ventral striatal area for post-stroke pain syndrome: a magnetoencephalography study. J. Neurophysiol. 119: 2118-2128.

Gramfort A, et al. (2013). MEG and EEG data analysis with MNE-Python. Front. Neurosci. 7: 267.

Green AL, Wang S, Stein JF, et al. (2009) Neural signatures in patients with neuropathic pain. Neurology 72: 569-571.

Grosenick, L., Marshel, J.H., Deisseroth, K (2015) Closed-loop and activity-guided optogenetic control. Neuron 86: 106-139.

Gross J, Schnitzler A, Timmermann L, Ploner M (2007). Gamma oscillations in human primary somatosensory cortex reflect pain perception. PLoS Biol. 5: e133.

Gu L, Uhelski ML, Anand S, Romero-Ortega M, Kim Y-t, Fuchs PN, et al. (2015) Pain Inhibition by Optogenetic Activation of Specific Anterior Cingulate Cortical Neurons. PLoS ONE 10: e0117746.

Guarnieri, R., Zhao, M., Taberna, G.A. et al. (2021). RT-NET: real-time reconstruction of neural activity using high-density electroencephalography. Neuroinform. 19: 251-266.

Guo X, Zhang Q, Singh A, Wang J, Chen Z. (2020). Granger causality analysis for rat cortical functional connectivity in pain. J. Neural Eng. 17: 016050.

Hastie T, Tibshirani R, Friedman J (2008) The Elements of Statistical Learning (2nd ed.). Springer (2008)

Hauck M, Lorenz J, Engel AK (2007). Attention to painful stimulation enhances gamma-band activity and synchronization in human sensorimotor cortex. J. Neurosci. 27: 9270-9277.

He H, Bai Y, Garcia EA, Li S (2008). ADASYN: adaptive synthetic sampling approach for imbalanced learning. Proc. IEEE Int. Joint. Conf. Neural Networks (IJCNN'08), pp. 1322-1328.

He H, Garcia EA (2009). Learning from imbalanced data. IEEE Trans. Knowledge and Data Engineering 21: 1263-1284.

Hecker L, Rupprecht R, Elst LT, Kornmeier J (2020).Convan vDip: Α convolutional neural network for better M/EEG imaging. source https://www.biorxiv.org/content/10.1101/2020.04.09.033506v1.full

Hillman EMC (2014) Coupling mechanism and significance of the BOLD signal: a status report. Ann. Rev. Neurosci. 37: 161-181.

Hnazaee MF, Wittevrongel B, Khachatryan E, et al. (2020) Localization of deep brain activity with scalp and subdural EEG. Neuroimage, 223: 117344.

Hsiao F-J, et al. (2020). Individual pain sensitivity is associated with resting-state cortical activities in healthy individuals but not in patients with migraine: a magnetoencephalography study. J. Headache Pain, 21, 133.

 ${
m Hu~L,~Iannetti~GD~(2016)}.$ Issues in pain prediction—beyond pain and gain. Trends Neurosci. 39: 640-642.

Hu L, Iannetti GD (2019). Neural indicators of perceptual variability of pain across species. Proc. Natl. Acad. Sci. USA 116: 1782-1791.

Hu S, Zhang Q, Wang J, Chen Z (2017) A real-time rodent neural interface for deciphering acute pain signals from neuronal ensemble spike activity, Proc. Asilomar Conf. Signals, Systems and Computers. IEEE Press (pp. 93–97)

Hu S, Zhang Q, Wang J, Chen Z (2018). Real-time particle filtering and smoothing algorithms for detecting abrupt changes in neural ensemble spike activity. J. Neurophysiol. 119: 1394-1410.

Huang G, Xiao P, Hung YS, Iannetti GD, Zhang ZG, Hu L (2013). A novel approach to predict subjective pain perception from single-trial laser-evoked potentials. Neuroimage 81: 283-293.

Huang Y, Luo H, Green AL, Aziz TZ, Wang S (2016) Characteristics of local field potentials correlate with pain relief by deep brain stimulation. Clin. Neurophysiol. 127: 2573-2580.

Huang G, Yu ZL, Liu K, et al. (2021). Electromagnetic source imaging via a data-synthesis-based denoising autoencoder. https://arxiv.org/pdf/2010.12876.pdf

Huang Y, Shang Q, Dai S, Ma Q (2017). Dread of uncertain pain: An event-related potential study. PLoS ONE 12(8): e0182489.

Hutchison WD, Davis KD, Lozano AM, Tasker RR, Dostrovsky JO (1999). Pain-related neurons in the human cingulate cortex. Nat. Neurosci. 2: 403-405.

Iannetti GD, Mouraux A (2010) From the neuromatrix to the pain matrix (and back). Exp. Brain Res., 205: 1-12.

Iannetti, G. D., Salomons, T. V., Moayedi, M., Mouraux, A., Davis, K. D. (2013) Beyond metaphor: contrasting mechanisms of social and physical pain. Trends Cogn. Sci. 17: 371-378.

Iannetti GD, Hughes NP, Lee MC, Mouraux A (2008). Determinants of laser-evoked EEG responses: pain perception or stimulus saliency? J. Neurophysiol. 100: 815-828.

Isnard J, Magnin M, Jung J, Mauguiere F, Garcia-Larrea L (2011). Does the insula tell our brain that we are in pain? Pain 152: 946-951.

Jabakhanji R, Vigotsky AD, Bielefeld J, Huang L, Baliki MN, Iannetti GD, Apkarian AV (2020) The hard limits of decoding mental states: The decodability of fMRI. https://doi.org/10.1101/2020.12.18.423495

Jas M, et al. (2017). Autoreject: automated artifact rejection for MEG and EEG data. Neuroimage 159: 417-429.

Jiang X, Bian G-B, Tian Z (2019) Removal of artifacts from EEG signals: a review. Sensors, 19: 987.

Jun JJ, Mitelut C, Lai C, et al. (2017). Real-time spike sorting platform for high-density extracellular probes with ground-truth validation and drift correction. https://www.biorxiv.org/content/10.1101/101030v1.

Kakigi R, Inui K, Tran DT, et al. (2004). Human brain processing and central mechanisms of pain as observed by electro- and magneto-encephalography. J. Chin. Med. Assoc. 67: 377-386.

Kano, M., Grinsvall, C., Ran, Q., Dupont, P., Morishita, J., Muratsubaki, T., Mugikura, S., Ly, H.G., Tornblom, H., Ljungberg, M., et al. (2020). Resting state functional connectivity of the pain

matrix and default mode network in irritable bowel syndrome: a graph theoretical analysis. Sci Rep 10: 11015.

Keefe FJ, Block AR (1982) Development of an observation method for assessing pain behavior in chronic low back pain patients. Behavior Therapy, 13: 363–375.

Kisler LB, Kim JA, Hemington KS, et al. (2020) Abnormal alpha band power in the dynamic pain connectome is a marker of chronic pain with a neuropathic component. Neuroimage: Clin. 26: 102241.

Knöpfel, T., Song, C. (2019) Optical voltage imaging in neurons: moving from technology development to practical tool. Nat. Rev. Neurosci. 20: 719-727.

Knotkova H, Hamani C, Sivanesan E, Le Beuffe MFE, Moon JY, Cohen SP, Huntoon MA (2021). Neuromodulation for chronic pain. Lancet, 397: 2111-2124.

Koepcke L, Ashida G, Kretzberg J (2016) Single and multiple change point detection in spike trains: Comparison of different CUSUM methods, Front. Syst. Neurosci. 10: 51.

Koles ZJ, Lazaret MS, Zhou SZ (1990) Spatial patterns underlying population differences in the background EEG. Brain Topography, 2: 275-284.

Koyama T, McHaffie JG, Laurienti PJ, Coghill RC (2005) The subjective experience of pain: Where expectations become reality. Proc Natl Acad Sci USA 102: 12950-12955.

Kucyi A, Davis KD (2017). The neural code for pain: from single-cell electrophysiology to the dynamic pain connectome. Neuroscientist 23: 397-414.

Kuner, R., Flor, H. (2016) Structural plasticity, connectivity and reorganisation in chronic pain. Nat. Rev. Neurosci. 18: 20-30.

Kuo CC, Yen CT (2005) Comparison of anterior cingulate and primary somatosensory neuronal responses to noxious laser-heat stimuli in conscious, behaving rats, J. Neurophysiol. 94, 1825-1836.

Kuo P-C, Chen Y-T, Chen Y-S, Chen l-F (2017). Decoding the perception of endogenous pain from rest-state MEG. Neuroimage 144: 1-11.

Kwan AC (2008). What can population calcium imaging tell us about neural circuits? J. Neurophysiol. 100: 977-980.

Kwon H, Choi YH, Lee JM (2019) A physarum centrality measure of the human brain network. Sci. Rep. 9: 5907.

Labus, J. S. et al. (2015) Multivariate morphological brain signatures predict patients with chronic abdominal pain from healthy control subjects. Pain 156: 1545-1554.

Lancaster J, Mano H, Callan D, Kawato M, Seymour B (2017). Decoding acute pain with combined EEG and physiological data. Proc. IEEE/EMBS Conf. Neural Eng. (NER), pp. 521-524.

Lecoq J, Orlova N, Grewe BF (2019) Wide. Fast. Deep. Recent advances in multi-photon microscopy of in vivo neuronal activity J. Neurosci., 39: 9042-9052.

Lee I-S, Necka EA, Atlas LY (2020) Distinguishing pain from nociception, salience, and arousal: How autonomic nervous system activity can improve neuroimaging tests of specificity. Neuroimage 204: 116254.

Lee J, Mawla I, Kim J, et al. (2019) Machine learning-based prediction of clinical pain using multimodal neuroimaging and autonomic metrics. Pain, 160: 550-560.

Lee M, Manders TR, Eberle SE, et al. (2015) Activation of corticostriatal circuitry relieves chronic neuropathic pain. J. Neurosci. 35: 5247-5259.

Leknes S, Berna C, Lee MC, et al. (2013) The importance of context: When relative relief renders pain pleasant. Pain, 154: 402-410.

Lenz FA, Rios M, Zirh A, Chau D, Krauss G, Lesser RP (1998). Painful stimuli evoke potentials recorded over the human anterior cingulate gyrus. J. Neurophysiol. 79: 2231-2234.

LeBlanc BW, Lii TR, Silverman AE, et al. (2014) Cortical theta is increased while thalamocortical coherence is decreased in rat models of acute and chronic pain. Pain 155: 773-782.

LeBlanc BW, Bowary PM, Chao Y-C, et al. (2016) Electroencephalographic signatures of pain and analgesia in rats. Pain 157: 2330-2340.

Li A, Liu Y, Zhang Q, et al. (2021) Disrupted population coding in the prefrontal cortex underlies pain aversion. Cell Rep., under revision.

Li Y, Murias, Major S, Dawson G, Dzirasa K, Carin L, Carlson DE (2017). Targeting EEG/LFP synchrony with neural nets. Advances in Neural Information Processing Systems 30. Long Beach, CA.

Liberati G, Klocker A, Algoet M, Mulders D, Safronova MM, Ferrao Santos S, et al. (2018). Gamma-band oscillations preferential for nociception can be recorded in the human insula. Cereb. Cortex 28: 3650-3664.

Liberati G, Klocker A, Safronova MM, Ferrao Santos S, Ribeiro Vaz JG, Raftopoulos C, et al. (2016). Nociceptive local field potentials recorded from the human insula are not specific for nociception. PLoS Biol. 14: e1002345.

Lim M, Kim JS, Kim DJ, Chung CK (2016) Increased low- and high-frequency oscillatory activity in the prefrontal cortex of fibromyalgia patients. Front. Hum. Neurosci. 10: 111.

Lopez-Martinez D, Peng K, Lee A, Borsook D, Picard R (2018) Pain detection with fNIRS-measured brain signals: a personalized machine learning approach using wavelet transform and Bayesian hierarchical modeling with Dirichlet process priors. Proc. Int. Conf. Affective Computing Intelligent Interaction. arXiv:1907.12830v1.

Lopez-Sola M, Woo C-W, Pujol J, et al. (2017) Towards a neurophysiological signature for fibromyalgia. Pain 158: 34-47.

Lotsch J, Ultsch A (2018) Machine learning in pain research. Pain 159: 623-630.

Lu C, Yang T, Zhao H, et al. (2016) Insular Cortex is Critical for the Perception, Modulation, and Chronification of Pain. Neurosci. Bull. 32: 191-201.

Macke JH, Buesing L, Sahani M (2015). Estimating state and parameters in state space models of spike trains. In Chen Z (Ed.): Advanced State Space Methods in Neural and Clinical Data. Cambridge University Press.

Malinen S, Vartiainen N, Hlushchuk Y, Koskinen M, Ramkumar P, Forss N, et al. (2010) Aberrant temporal and spatial brain activity during rest in patients with chronic pain. Proc Natl Acad Sci USA 107: 6493-6497.

May ES, Nickel MM, et al. (2019). Prefrontal gamma oscillations reflect ongoing tonic back pain patients. Hum. Brain Mapp. 40: 293-305.

Meda KS, Patel T, Braz JM, et al. (2019) Microcircuit mechanisms through which mediodorsal thalamic input to anterior cingulate cortex exacerbates pain-related aversion. Neuron, 102: 944-959.

Melzack R, Casey KL (1968) Sensory, motivational, and central control determinants of pain: A new conceptual model. In Kenshalo D (editor), *The Skin Senses* (pp. 423-443), Charles C. Thomas, Publisher.

Mickle, A.D., et al. (2019) A wireless closed-loop system for optogenetic peripheral neuromodulation. Nature 565: 361-365.

Moayedi M, Salomons TV, Atlas LY (2018) Pain neuroimaging in humans: A primer for beginners and non-imagers. J. Pain, 19: e1-e21.

Morton DL, Sandhu JS, Jones AKP (2016) Brain imaging of pain: state of the art. J. Pain Res. 9: 613-624.

Mouraux A, Iannetti GD (2009). Nociceptive laser-evoked brain potentials do not reflect nociceptive-specific neural activity. J. Neurophysiol. 101: 3258-3269.

Mouraux A, Iannetti GD (2018). The search for pain biomarkers in the human brain. Brain 141: 3290-3307.

Murphy KP (2012) Machine Learning: A Probabilistic Perspective. Cambridge, MA: MIT Press.

Nason, S.R., Vaskov, A.K., Willsey, M.S. et al. (2020) A low-power band of neuronal spiking activity dominated by local single units improves the performance of brain-machine interfaces. Nat Biomed Eng 4: 973-983.

Necka EA, Lee I-S, Kucyi A, et al. (2019) Applications of dynamic functional connectivity to pain and its modulation. Pain Rep. 4: e752.

Nickel MM, Dinh ST, May ES, et al. (2020). Neural oscillations and connectivity characterizing the state of tonic experimental pain in humans. Hum. Brain Mapp. 41: 17-29.

Pachitariu M, Steinmetz N, Kadir S, Carandini M and Harris KD (2016). Kilsort: real-time spike-sorting for extracellular electrophysiology with hundreds of channels. https://www.biorxiv.org/content/10.1101/061481v1.

Pachitariu M, Stringer C, Harris KD (2018). Robustness of spike deconvolution for neuronal calcium imaging. J. Neurosci. 38: 7976-7985.

Parvizi, J., Kastner, S. (2018) Promises and limitations of human intracranial electroencephalography. Nat Neurosci 21: 474-483.

Pesaran, B., Vinck, M., Einevoll, G.T. et al. (2018) Investigating large-scale brain dynamics using field potential recordings: analysis and interpretation. Nat Neurosci 21: 903-919.

Phelps CE, Navratilova E, Porreca F (2021). Cognition in the chronic pain experience: Preclinical insights. Trends Cog. Sci. 25: 365-376.

Pinheiro ES, de Queiros FC, Montoya P, et al. (2016) Electroencephalographic patterns in chronic pain: a systematic review of the literature. PLoS ONE 11: e0149085.

Ploghaus A, Tracey I, Gati JS, Clare S, Menon RS, Matthews PM, et al. (1999). Dissociating pain from its anticipation in the human brain. Science, 284: 1979-1981.

Ploner M, Schoffelen J-M, Schnitzler A, Gross J (2009). Functional integration within the human pain system as revealed by Granger causality. Hum. Brain Mapp. 30: 4025-4032.

Ploner M, Sorg C, Gross J (2017). Brian rhythms of pain. Trends Cog. Sci. 21: 100-110.

Ploner M, May ES (2017). Electroencephalography and magnetoencephalography in pain research—current state and future perspectives. Pain 159: 206-211.

Pnevmatikakis, E.A., Soudry, D., Gao, Y., et al. (2016). Simultaneous denoising, deconvolution, and demixing of calcium imaging data. Neuron 89: 285-299.

Poldrack R. A., Huckins G., Varoquaux G. (2020) Establishment of best practices for evidence for prediction: a review. JAMA Psychiatry, 77: 534-540.

Prkachin KM, Berzins S, Mercer SR (1994) Encoding and decoding of pain expressions: a judgement study. Pain, 58: 253-259.

Raduntz T, Scouten J, Hochmuch O, Meffert B (2015) EEG artifact elimination by extraction of ICA-component features using image processing algorithms. J. Neurosci. Methods 243: 84-93.

Rainville P, Duncan GH, Price DD, Carrier B, Bushnell MC (1997). Pain affect encoded in human anterior cingulate but not somatosensory cortex. Science 277: 968-971.

Rasmussen CE, Williams CKI (2009). Gaussian Processes for Machine Learning. MIT Press.

Reckziegel D, Vachon-Presseau E, Bogdan P, et al. (2019) Deconstructing biomarkers for chronic pain: context- and hypothesis-dependent biomarker types in relation to chronic pain. Pain, 160: S37-S48.

Rosa MJ, Seymour B (2014) Decoding the matrix: benefits and limitations of applying machine learning algorithms to pain neuroimaging. Pain, 155: 864-867.

Sarnthein J, Stern J, Aufenberg C, Rousson V, Jeanmonod D (2006). Increased EEG power and slowed dominant frequency in patients with neurogenic pain. Brain 129: 55-64.

Sawamoto N, Honda M, Okada T, et al. (2000) Expectation of pain enhances responses to non-painful somatosensory stimulation in the anterior cingulate cortex and parietal operculum/posterior insula: an event-related functional magnetic resonance imaging study. J. Neurosci. 20: 7438-7445.

Schouppe S, van Oostyerwijck S, Danneels L, et al. (2020) Are functional brain alterations present in low back pain? A systematic review of EEG studies. J. Pain 21: 25-43.

Schulz E, Zherdin A, Tiemann L, Plant C, Ploner M (2012). Decoding an individual's sensitivity to pain from the multivariate analysis of EEG data. Cereb. Cortex 22: 118-123.

Schulz E, May ES, Postorino M, Tiemann L, Nickel MM, Witkovsky V, Schmidt P, Gross J, Ploner M (2015). Prefrontal gamma oscillations encode tonic pain in humans. Cereb. Cortex 25: 4407-4414.

Seeber, M., Cantonas, LM., Hoevels, M. et al. (2019) Subcortical electrophysiological activity is detectable with high-density EEG source imaging, Nat. Commun. 10: 753.

Senkowski D, Hófle M, Engel AK. (2014) Crossmodal shaping of pain: A multisensory approach to nociception. Trends Cogn. Sci., 18: 319-327.

Shanechi MM (2019). Brain-machine interfaces from motor to mood. Nat. Neurosci. 22: 1554-1564.

Shirvalkar P, Veuthey TL, Dawes HE, Chang EF (2019). Closed-loop deep brain stimulation for refractory chronic pain. Front. Comp. Neurosci. 12: 18.

Singh A, Patel D, Hu L, Li A, Zhang Q, Guo X, Robinson E, Martinez E, Doan L, Rudy B, Chen Z, Wang J (2020). Mapping cortical integration of sensory and affective pain pathways. Curr. Biol. 30: 1703-1715.

Spisak, T., Kincses, B., Schlitt, F., Zunhammer, M., Schmidt-Wilcke, T., Kincses, Z.T., and Bingel, U. (2020). Pain-free resting-state functional brain connectivity predicts individual pain sensitivity. Nat Commun 11: 187.

Sporns, O., Tononi, G., Kotter, R (2005) The human connectome: A structural description of the human brain. PLoS Comput. Biol. 1: e42.

Starr CJ, Sawaki L, Wittenberg GF, et al. (2009) Roles of the Insular Cortex in the Modulation of Pain: Insights from Brain Lesions, J. Neurosci. 29: 2684-2694.

Stern J, Jeanmonod D, Sarnthein J (2006). Persistent EEG overactivation in the cortical pain matrix of neurogenic pain patients. Neuroimage 31: 721-731.

Stober S, Sternin A, Owen AM, Grahn JA (2016). Deep feature learning for EEG recordings. Proc. International Conf. learned Representations (ICLR'16). https://arxiv.org/abs/1511.04306

Sun G, Wen Z, Ok D, Doan L, Wang J, Chen Z (2021a). Detecting acute pain signals from human EEG. J. Neurosci. Methods, 347: 108964.

Sun G, Zen F, Zhang Q, Liu Y, Chen Z, Wang J (2021b). A multi-region neural interface provides analgesia. Under review.

Tan, L.L., Oswald, M.J., Heinl, C. et al. (2019). Gamma oscillations in somatosensory cortex recruit prefrontal and descending serotonergic pathways in aversion and nociception. Nat. Commun. 10: 983.

Tayeb, Z., Bose, R., Dragomir, A. et al. (2020). Decoding of pain perception using EEG signals for a real-time reflex system in prostheses: a case study. Sci. Rep. 10: 5606.

Tiemann L, Hohn VD, Ta Dinh S, May ES, Nickel MM, Gross J, Ploner M. (2018). Distinct patterns of brain activity mediate perceptual and motor and autonomic responses to noxious stimuli. Nat. Commun. 9: 4487.

Tøttrup L, Atashzar SF, Farina D, et al. (2021). Altered evoked low-frequency connectivity from SI to ACC following nerve injury in rats. J. Neural Eng. 18: 046063.

Tu Y, Tan A, Bai Y, Hung Y S, Zhang Z (2016). Decoding subjective intensity of nociceptive pain from pre-stimulus and post-stimulus brain activities. Front. Comp. Neurosci. 10: 32.

Ung H, Brown JE, Johnson KA, Younger J, Hush J, Mackey S (2014) Multivariate classification of structural MRI data detects chronic low back pain. Cereb. Cortex, 24: 1037-1044.

Urien L, Xiao Z, Dale J, et al. (2018). Rate and temporal coding mechanisms in the anterior cingulate cortex for pain anticipation. Sci. Rep. 8: 8298.

Vachon-Presseau, E., Berger, S.E., Abdullah, T.B., Griffith, J.W., Schnitzer, T.J., and Apkarian, A.V. (2019). Identification of traits and functional connectivity-based neurotraits of chronic pain. PLoS Biol 17: e3000349.

van der Miesen MM, Lindquist MA, Wager TD (2019). Neuroimaging-based biomarkers for pain: state of the field and current directions. PAIN Reports 4: e751.

Varoquaux, G (2018). Cross-validation failure: small sample sizes lead to large error bars. Neuroimage 180: 68-77.

Vecchio F, Miraglia F, Rossini PM (2017) Connectome: Graph theory application in functional brain network architecture. Clinical Neurophysiology Practice, 2: 206-213.

Vierck CJ, Whitsel BL, Favorov OV, Brown AW, Tommerdahl M (2013). Role of primary somatosensory cortex in the coding of pain. Pain 154: 334-344.

Vijayakumar V, Case M, Shirinpour S, He B (2017) Quantifying and characterizing tonic thermal pain across subjects from EEG data using random forest models. IEEE Trans. Biomed. Eng. 64: 2988–2966.

Wager TD, Atlas LY, Lindquist MA, Roy M, Woo CW, Kross E (2013). An fMRI-based neurologic signature of physical pain. N. Engl. J. Med. 368: 1388-1397.

Wang J, Wang J, Xing GG, LI X, Wan Y (2016). Enhance gamma oscillatory activity in rats with chronic inflammatory pain. Front. Neurosci. 10: 489.

Wei C, Lou K, Wang Z, et al. (2021). Edge sparse basis network: A deep learning framework for EEG source localization. https://arxiv.org/pdf/2102.09188.pdf

Wei Z, Lin B-J, Chen T-W, Daie K, Svoboda K, Druckmann S (2020) A comparison of neuronal population dynamics measured with calcium imaging and electrophysiology. PLoS Comput Biol 16: e1008198.

Wiech K, Ploner M, Tracey I (2008) Neurocognitive aspects of pain perception. Trends Cog. Sci. 12: 306-313.

Willis WD, Westlund KN (1997) Neuroanatomy of the pain system and of the pathways that modulate pain. Clin Neurophysiol. 14: 2-31.

Woo, C. W., Chang, L. J., Lindquist, M. A., Wager, T. D. (2017) Building better biomarkers: brain models in translational neuroimaging. Nat. Neurosci. 20: 365-377.

Wu W, Chen Z, Gao S, Brown EN (2011). A hierarchical Bayesian approach for learning spatiotemporal decomposition of multichannel EEG. Neuroimage, 56: 1929-1945.

Wu W, Wu C, Gao S, Liu B, Li Y, Gao X (2013). Bayesian estimation of ERP components from multicondition and multichannel EEG. Neuroimage, 88: 319-339.

Wu W, Chen Z, Gao X, Li Y, Brown EN, Gao S (2015). Probabilistic common spatial patterns for multichannel EEG analysis. IEEE Trans. Pattern Analysis Machine Intelligence, 37: 639-653.

Wu W, Nagarajan S, Chen Z (2016) Bayesian machine learning for EEG/MEG signal processing measurements. IEEE Signal Processing Magazine, 33: 15-36.

Xiao Z, Hu S, Zhang Q, Tian X, Chen W, Wang J, Chen Z (2019). Ensembles of change-point detectors: implications for real-time BMI applications. J. Comput. Neurosci. 46: 107-124.

Xiao Z, Martinez E, et al. (2019) Cortical pain processing in the rat anterior cingulate cortex and primary somatosensory cortex. Front. Cell. Neurosci. 13: 165.

Xu Q, Dong X (2019) Calcium imaging approaches in investigation of pain mechanism in the spinal cord. Exp. Neurol. 317: 129-132.

Yger P, Spampinato GLB, Esposito E, et al. (2018). A spike sorting toolbox for up to thousands of electrodes validated with ground truth recordings in vitro and in vivo. eLife 7: e34518.

Zhang Q, Manders T, Tong APS, Yang R, Garg A, Martinez E, Goyal A, Dale J, Zhou H, Urien L, Sideris A, Yang G, Chen Z, Wang J (2017) Chronic pain induces generalized enhancement of aversion to noxious inputs. eLife, 6: e25302.

Zhang Q, Xiao Z, Huang C, Hu S, Kulkarni P, Martinez E, Tong AP, Garg A, Chen Z, Wang J (2018) Local field potential decoding of the onset and intensity of acute pain in rats. Sci. Rep. 8: 1-11.

Zhang Q, Hu S, Talay R, Xiao Z, Rosenberg D, Li A, Caravan B, Liu Y, Sun G, Singh A, Gould JD, Chen Z, Wang J (2021). A prototype closed-loop brain-machine interface for the study and treatment of pain. Nat. Biomed. Eng., https://doi.org/10.1038/s41551-021-00736-7

Zhang S, Yoshida W, Mano H, et al. (2020). Pain control by co-adaptive learning in a brain-machine interface. Curr. Biol. 30: 1-10.

Zhang ZG, Hu L, Hung YS, Mouraux A, Iannetti GD (2012) Gamma-band oscillations in the primary somatosensory cortex—a direct and obligatory correlate of subjective pain intensity. J. Neurosci. 32: 7429-7438.

Zhou R, Wang J, Qi W, Liu F-Y, Yi M, Guo H, Wan Y (2018). Elevated resting state gamma oscillatory activities in electroencephalogram of patients with post-herpetic neuralgia. Front. Neurosci. 12: 750.

Zhou H, Zhang Q, Martinez E, Dale J, et al. (2019). A novel neuromodulation strategy to enhance the prefrontal control to treat pain. Mol. Pain, 15: 1744806919845739.

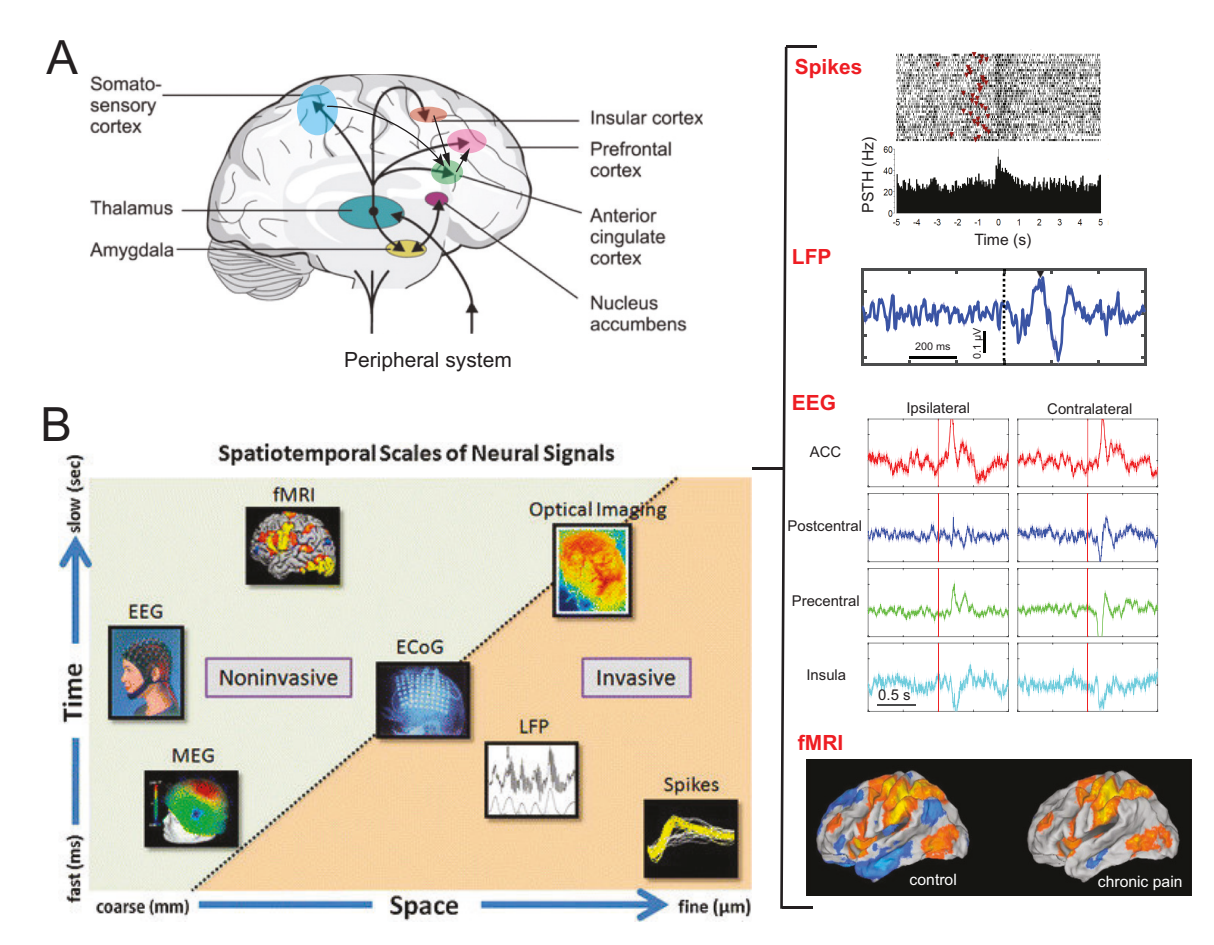


Figure 1: (A) A schematic illustration of distributed cortical-subcortical pain areas. (B) Comparison of spatial and temporal resolution of brain signals (from Chen, 2017; reproduced with permission, ©IEEE). On the right, panels from top to bottom panels show pain-modulated single-unit spike raster of rat ACC (from Chen et al., 2017b; reproduced with permission, ©IOP press), pain-evoked ERP from a rat LFP signal, pain-evoked ERP from source-localized human EEG signals (from Sun et al., 2021a; reproduced with permission, ©Elsevier), and human neuroimaging.

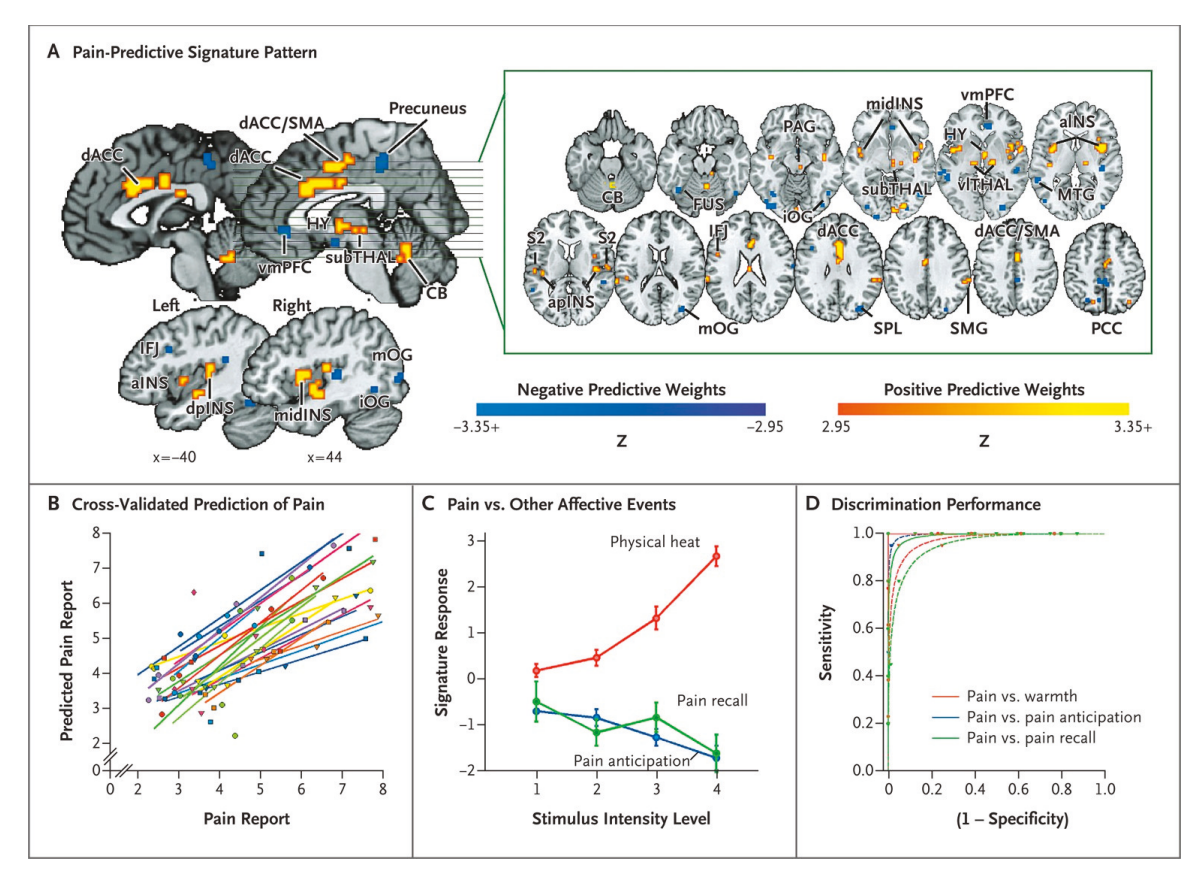


Figure 2: (A) Pain-predictive signature pattern in human fMRI study. Color-coded voxels show the brain area whose activity reliably predicted pain. The map shows weights that exceed a threshold (a false discovery rate of <0.05) for display only; all weights were used in prediction. (B) Comparison of pain report and cross-validated predicted pain. Each colored line or symbol represents an individual participant. (C) Signature response versus the pain intensity for heat, pain-anticipation, and pain-recall conditions. (D) The receiver-operating-characteristic (ROC) plots in classification of pain (Wager et al., 2013; reproduced with permission, ©Massachusetts Medical Society).

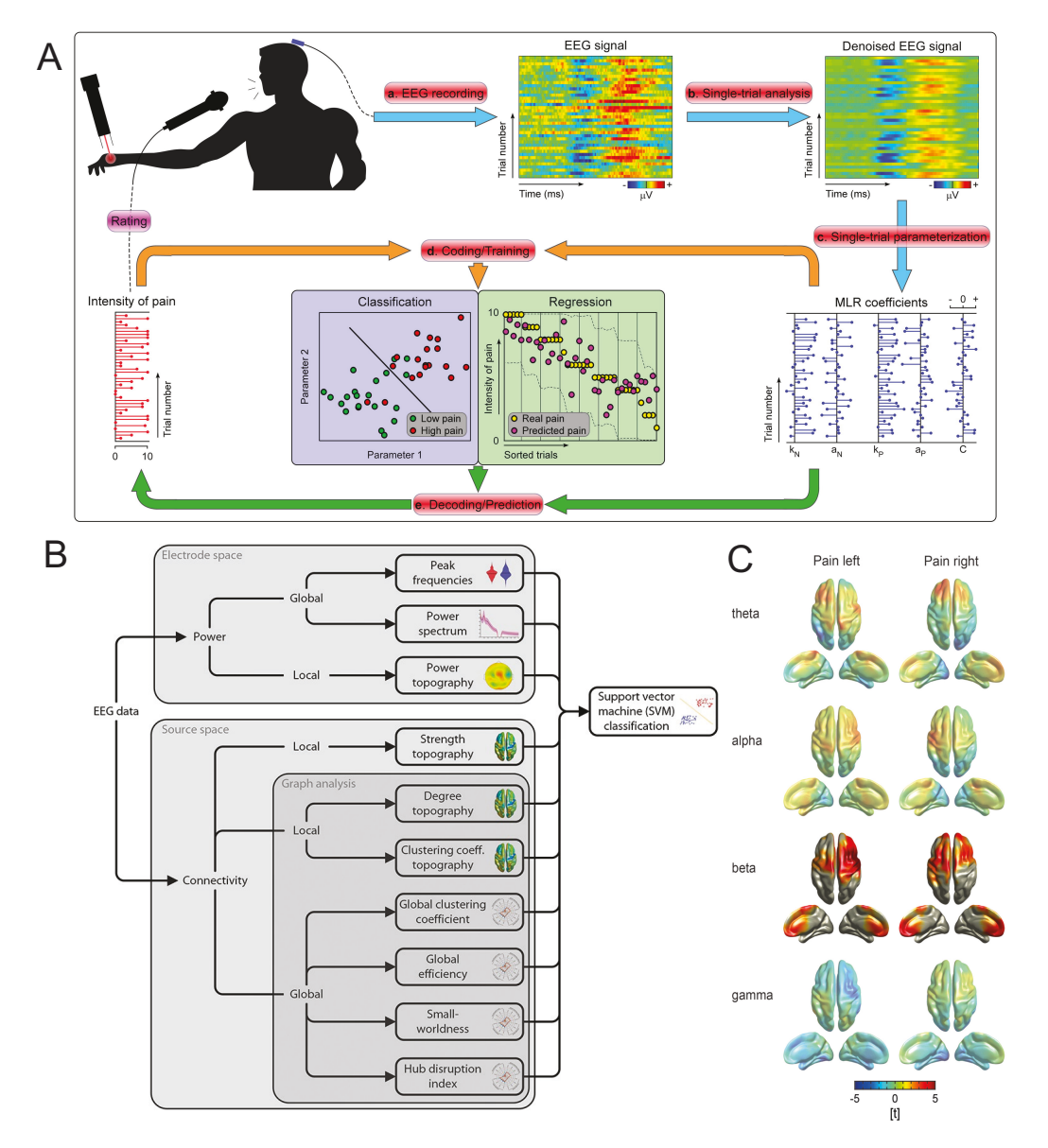


Figure 3: (A) EEG-based subjective pain prediction based on common spatial pattern (CSP) and machine learning. The relationship between multiple linear regression (MLR) coefficients and intensity of pain perception on a single-trial basis can be trained using both classification and regression approaches (Huang et al., 2013; reproduced with permission, ©Elsevier). (B) EEG data analysis pipeline at both electrode space and source space. Different features are extracted based on local and global brain activity (Dinh et al., 2019; reproduced with permission, ©International Association for the Study of Pain). (C) Visualization of EEG-inferred functional connectivity of brain between pain and control conditions. Strength of connectivity of each voxel was computed by averaging the connectivity, as measured by the phase locking value (PLV), of each voxel to all other voxels. Warm and cold colors indicate increased and decreased strength of connectivity in the pain condition as compared to the control condition, respectively. In the beta frequency band, connectivity was increased in both pain conditions predominantly contralateral to the stimulated hand (Nickel et al., 2020; reproduced with permission, ©Wiley).

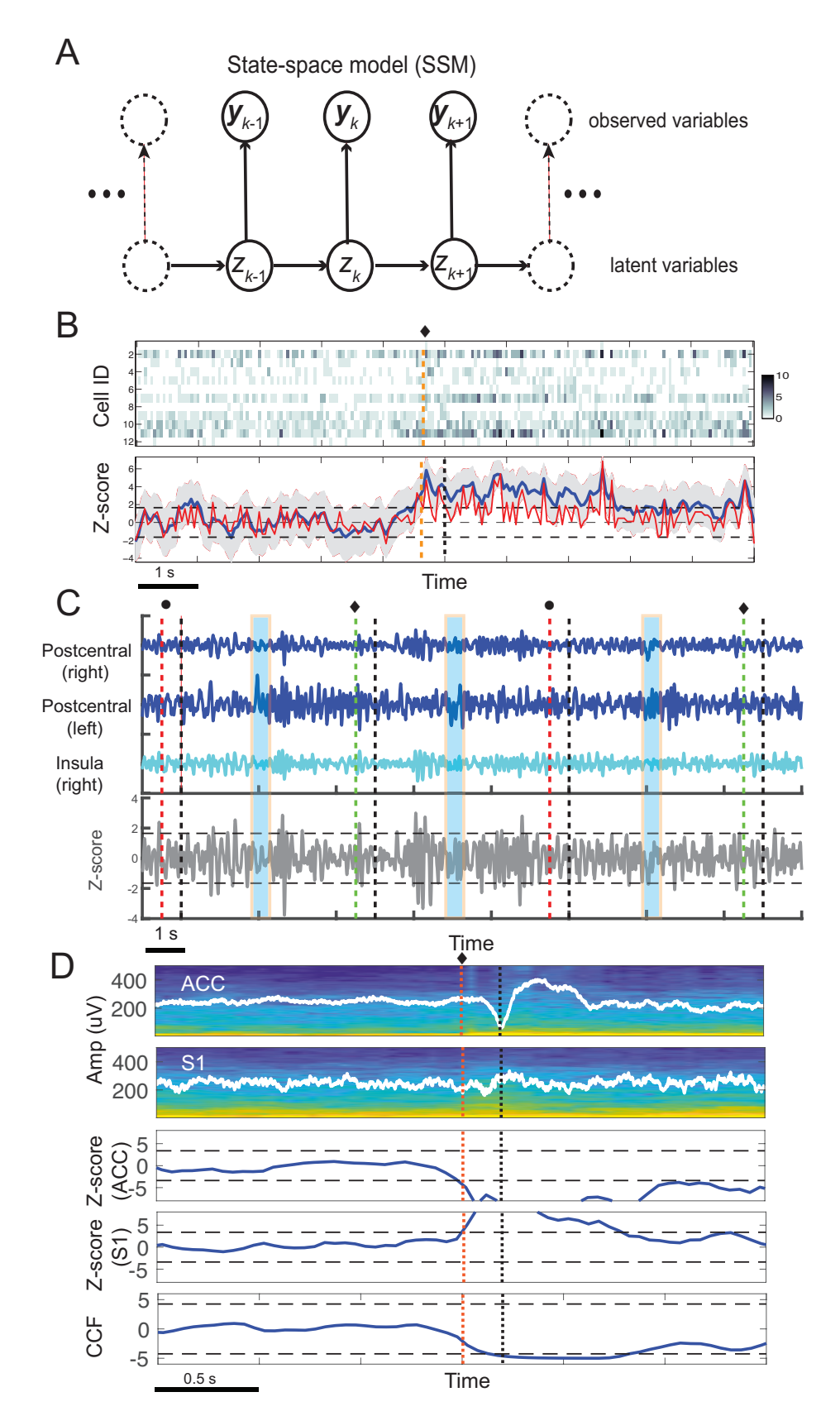


Figure 4: (A) A schematic diagram of state-space model (SSM). The latent variables $\{z_k\}$ are drawn from a linear Gaussian-Markov process, which modulates the observed random variables $\{\mathbf{y}_k\}$, which can be either Poisson or Gaussian distributed. (B-D) SSM-based approaches for detecting acute pain signals based on (B) simultaneously recorded spike trains of neuronal ensembles (adapted from Chen et al., 2017b; reproduced with permission, ©IOP press), (C) EEG source-localized temporal traces (adapted from Sun et al., 2021; reproduced with permission, ©Elsevier), and (D) simultaneous LFP recordings from the rat ACC and S1. Horizontal dashed lines denote the significance threshold. black dotted line denotes the paw or hand withdrawal. Red or green vertical dotted line denotes either non-noxious (\bullet) or noxious (\bullet) stimulus onset.

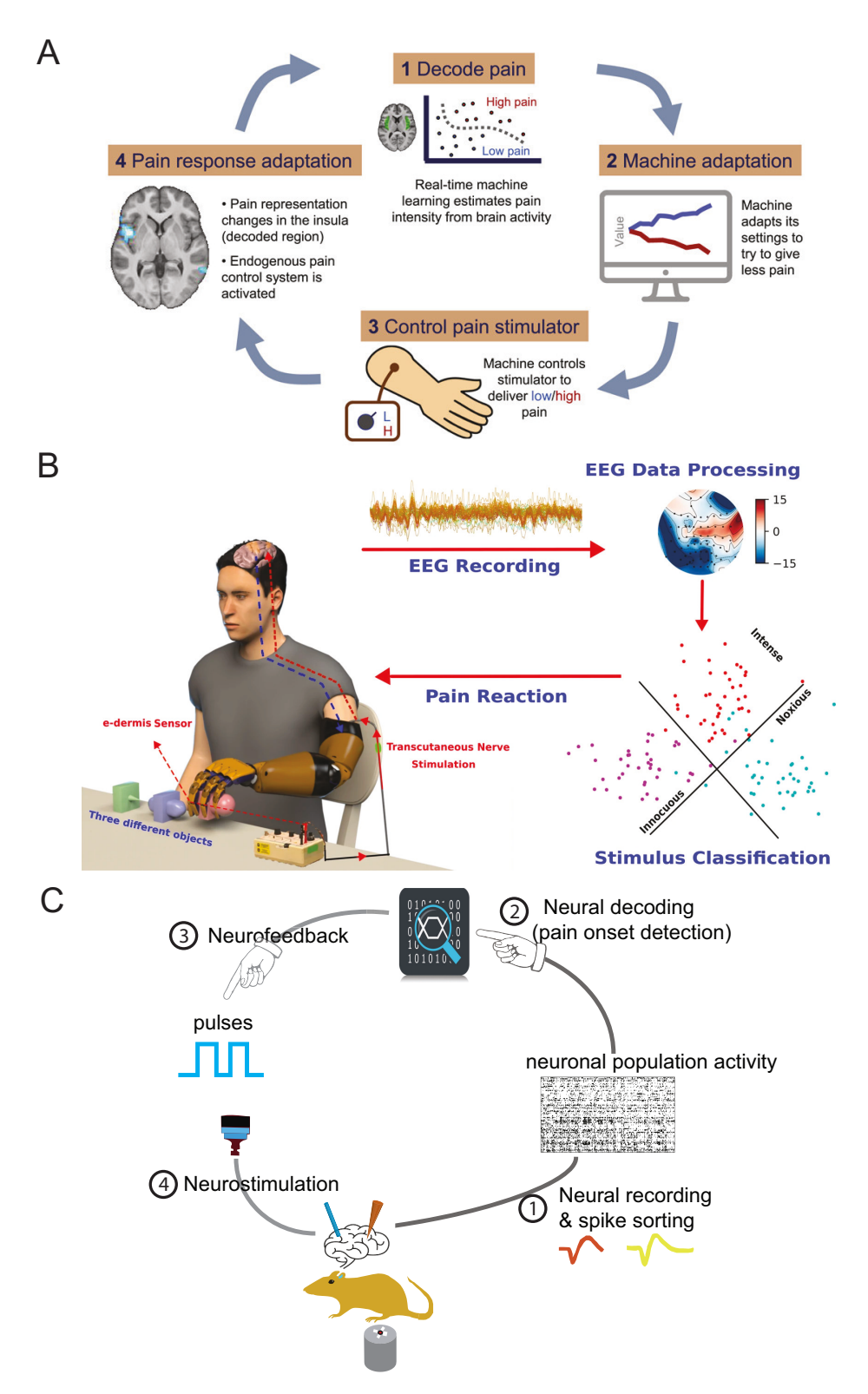


Figure 5: (A) A schematic of real-time BMI for pain control (Zhang et al., 2020; reproduced with permission, ©Elsevier). (B) An EEG-based system implementation overview of a prosthetic arm that can restore the sense of touch and pain (Tayeb et al., 2020; reproduced with CC BY license). (C) A schematic diagram of closed-loop rodent BMI for pain detection and neurostimulation (Zhang et al., 2021; reproduced with permission, ©Nature Springer).